FINITE ELEMENT MODELLING OF LINEAR ROLLING CONTACT PROBLEMS

ESAIM: M2AN 58 (2024) 1541–1579
https://doi.org/10.1051/m2an/2024052

ESAIM: Mathematical Modelling and Numerical Analysis
www.esaim-m2an.org

FINITE ELEMENT MODELLING OF LINEAR ROLLING CONTACT PROBLEMS

Luigi Romano[1,*] and Axel Målqvist[2]

Abstract. The present work is devoted to the finite element modelling of linear hyperbolic rolling contact problems. The main equations encountered in rolling contact mechanics are reviewed in the first part of the paper, with particular emphasis on applications from automotive and vehicle engineering. In contrast to the common hyperbolic systems found in the literature, such equations include integral and boundary terms, as well as time-varying transport velocities, that require special treatment. In this context, existence and uniqueness properties are discussed within the theoretical framework offered by the semigroup theory. The second part of the paper is then dedicated to recovering approximated solutions to the considered problems, by combining discontinuous Galerkin finite element methods (DGMs) with explicit Runge–Kutta (RK) schemes of the first and second order for time discretisation. Under opportune assumptions on the smoothness of the sought solutions, and owing to certain generalised Courant–Friedrichs–Lewy (CFL) conditions, quasi-optimal error bounds are derived for the complete discrete schemes. The proposed algorithms are then tested on simple scalar equations in one space dimension. Numerical experiments seem to suggest the theoretical error estimates to be sharp.

Mathematics Subject Classification. 35L02, 35L04, 35Q49, 65M06, 65M08, 65M12, 65M60, 74A55, 74H15, 74H20, 74H25.

Received September 21, 2023. Accepted June 26, 2024.

1. Introduction

Linear hyperbolic partial differential equations (PDEs) are ubiquitous in physics and engineering [1,2]. Particularly, in the field of contact mechanics, hyperbolic PDEs appear in numerous applications concerning rolling contact phenomena, where they typically describe the complex interactions occurring between wheel and rail [3–6], tyre and road asphalt [7,8], but also the dynamics of roll bearing elements, belt-pulley mechanisms, and continuous automotive transmissions [9–11]. Especially in vehicle engineering, the most common formulations adopt brush-like representations of the contacting rolling bodies [12,13], where dry friction is modelled according to the famous Coulomb-Amontons theory [14–16]. Advanced descriptions based on modified friction theories, such as the LuGre-brush model [17–25], are also able to accurately account for wet and lubricated friction and have been successfully employed for control design. In one space dimension, a typical example of hyperbolic

Keywords and phrases. Rolling contact mechanics, hyperbolic rolling contact problems, numerical modelling, discontinuous Galerkin finite element methods (DGMs), Runge–Kutta schemes.

[1] Division of Vehicular Systems, Department of Electrical Engineering, Linköping University, SE-581 83 Linköping, Sweden.

[2] Department of Mathematical Sciences, Chalmers University of Technology and University of Gothenburg, Chalmers Tvärgata 3, 412 58 Gothenburg, Sweden.

*Corresponding author: luigi.romano@liu.se

PDEs encountered in rolling contact mechanics is as follows:

$$\frac{\partial u(x,t)}{\partial t} + a(x,t)\,\frac{\partial u(x,t)}{\partial x} = B(t)u(x,t) + C(t)u(1,t) + f(x,t), \qquad \text{for } (x,t) \in (0,1)\times(0,T), \tag{1a}$$

$$u(0,t) = 0, \qquad \text{for } t \in (0,T), \tag{1b}$$

$$u(x,0) = u_0(x), \qquad \text{for } x \in (0,1), \tag{1c}$$

where $u(x,t) \in \mathbb{R}^n$ is the unknown solution, measuring a tangential deformation, $a(x,t) \in \mathbb{R}$ denotes the transport velocity, $f(x,t) \in \mathbb{R}^n$ is the external forcing term, and $C(t)$ and $B(t)$ are bounded operators.

Whilst numerous analytical steady-state models allowing for simple closed-form solutions may be encountered in the dedicated literature, the accurate modelling of certain physical phenomena requires taking into account unsteady effects. When it comes to simulating the behaviour of many engineering systems, this implies the need to solve the underlying PDEs numerically, which has limited the deal of effort devoted to such investigations. Restricting the attention to the field of railway dynamics, departing from the theory developed by Kalker [26,27], the currently available numerical methods including commercial software like FASTSIM® and CONTACT® employ variational techniques to iteratively solve the transient problem until convergence is achieved [28–31]. Albeit being sufficiently accurate for the purpose they serve, such algorithms cannot be easily extended to cover problems arising from other subfields of vehicle engineering and contact mechanics [32,33], which may instead be studied using finite element methods. In this context, the present paper is devoted to the numerical modelling of linear rolling contact phenomena, by combining PDE-based formulations with discontinuous Galerkin finite element methods (DGMs) for space approximation [34–37]. Since the ultimate ambition is to develop numerical algorithms (or extensions thereof) enabling fast calculations with performance close to real-time requirements, and easily implementable in virtual environments like MATLAB/Simulink®, time discretisation is then achieved using explicit schemes. More specifically, first and second-order Runge–Kutta (RK) algorithms, which represent a sufficiently good compromise between accuracy and computational speed [38,39], are mainly explored in the present work. To the author's best knowledge, the numerical methods developed in this paper also constitute a novelty concerning the modelling of linear rolling contact phenomena described by brush-like formulations.

From the perspective of the pure mathematical analysis, the approach pursued in this paper is heavily inspired by the research carried out in [38,39], where the authors have rigorously investigated the rate of convergence of different finite element methods (FEMs) in conjunction with explicit RK schemes up to the third order, using arguments based on energy estimates. However, the techniques developed in [38,39] are not directly applicable to most of the initial-boundary-value problems (IBVPs) appearing in rolling contact mechanics and considered in the following, since the PDEs describing rolling contact phenomena may contain integral and boundary terms whose presence has not been accounted for in previous studies. Additionally, handling time-varying data requires modifications of the analyses conducted in [38,39], since the corresponding discrete equations for the error dynamics cannot be cast in the same form as that considered in [38,39]. Therefore, the present work also delivers some results concerning the mathematical analysis of DGMs combined with RK algorithms. In this context, it should be also mentioned that the techniques presented in this paper may be extended to the study of other interesting problems arising from different branches of physics and engineering. For example, typical equations that may be covered by the results advocated in the present work include those treated in [40].

In particular, the remainder of the manuscript is organised as follows. In Section 2, the general structure for the considered hyperbolic PDEs is outlined concerning the one-dimensional and multi-dimensional cases. Under certain assumptions, the existence and uniqueness of such equations are established according to the semigroup theory. Section 3 introduces the space semi-discretisation approach, which enables recovering approximated solutions to the considered initial-boundary-value problems (IBVPs) within finite-dimensional polynomial spaces. More specifically, this is accomplished by replacing the continuous operator appearing in the abstract formulation with a discrete counterpart, whose salient properties are investigated in detail. Then, Section 4 introduces the complete discrete schemes, which cover explicit RK algorithms of the first and second order (RK1 and RK2, respectively). Owing to certain refined Courant–Friedrichs–Lewy (CFL) conditions, convergence results for the

complete discrete schemes are asserted under the assumption of sufficiently smooth exact solutions. In particular, the analysis is fully detailed concerning the RK2 algorithms presented in the paper (some technical result are more appropriately collected in Appendix A). In Section 5, numerical experiments concerning the error convergence are conducted considering both smooth and less regular solutions. Finally, the main conclusions, together with some directions for future research, are summarised in Section 6.

2. Linear problems in rolling contact mechanics

The present section reviews the main hyperbolic problems encountered in rolling contact mechanics, for which existence and uniqueness may be established using a semigroup approach.

2.1. Preliminaries and notation

In this paper, the set of real numbers is indicated with $\mathbb{R}$; $\mathbb{R}_{>0}$ and $\mathbb{R}_{\geq 0}$ denote the set of positive real numbers and positive real numbers including zero, respectively. The sets of natural numbers excluding and including zero are indicated with $\mathbb{N}$ and $\mathbb{N}_0$.

Generic Banach spaces are conventionally denoted by X (respectively Y), and equipped with norm $\|\cdot\|_X$ (respectively $\|\cdot\|_Y$); the identity operator is denoted by I_X (respectively I_Y). Similarly, generic Hilbert spaces are indicated with V, and equipped with inner product $\langle\cdot,\cdot\rangle_V$ and norm $\|\cdot\|_V$. The corresponding identity operator is I_V (when no ambiguity arises, the subscript might be omitted for brevity). Specifically, given a domain $\Omega \subset \mathbb{R}^d$, the Hilbert space $L^2(\Omega;\mathbb{R}^n)$ is endowed with inner product and induced norm

$$\langle v, w\rangle_{L^2(\Omega;\mathbb{R}^n)} \triangleq \int_\Omega v(x)\cdot w(x)\,\mathrm{d}x = \int_\Omega v^{\mathrm{T}}(x)w(x)\,\mathrm{d}x, \tag{2a}$$

$$\|v(\cdot)\|^2_{L^2(\Omega;\mathbb{R}^n)} \triangleq \langle v, v\rangle_{L^2(\Omega;\mathbb{R}^n)} = \int_\Omega \|v(x)\|_2^2\,\mathrm{d}x, \tag{2b}$$

where $\|\cdot\|_2$ denotes the standard Euclidean norm in $\mathbb{R}^n$, respectively. A function $v(\cdot)$ is said to belong to the space $L^2(\Omega;\mathbb{R}^n)$, noted $v \in L^2(\Omega;\mathbb{R}^n)$, if its L^2-norm defined according to equation (2b) is finite. Similarly, the Hilbert space $H^1(\Omega;\mathbb{R}^n)$ is naturally equipped with seminorm and norm

$$|v(\cdot)|^2_{H^1(\Omega;\mathbb{R}^n)} \triangleq \sum_{i=1}^{n} \|\nabla v_i(\cdot)\|^2_{L^2(\Omega;\mathbb{R}^d)}\,, \tag{3a}$$

$$\|v(\cdot)\|^2_{H^1(\Omega;\mathbb{R}^n)} \triangleq \|v(\cdot)\|^2_{L^2(\Omega;\mathbb{R}^n)} + |v(\cdot)|^2_{H^1(\Omega;\mathbb{R}^n)}\,. \tag{3b}$$

A function $v(\cdot)$ is said to belong to the space $H^1(\Omega;\mathbb{R}^n)$, noted $v \in H^1(\Omega;\mathbb{R}^n)$, if its H^1-norm as in equation (3b) is finite.

The Banach space $C^0(\overline{\Omega};\mathbb{R}^n)$ is also endowed with norm

$$\|v(\cdot)\|_\infty \triangleq \max_{\overline{\Omega}} \|v(x)\|_2\,. \tag{4}$$

Concerning a function $v(\cdot,\cdot)$ defined on the space-time cylinder $\Omega\times(0,T)$, it is often convenient to interpret $v(\cdot)$ as a function of the time variable with values in a Banach space X, spanned by functions of the space variables, *i.e.*,

$$v : (0,T) \ni t \mapsto v(t) \equiv v(\cdot,t) \in X. \tag{5}$$

For any integer $l \in \mathbb{N}_0$, the spaces $C^l([0,T];X)$ are also considered, spanned by functions that are l times continuously differentiable in the interval $[0,T]$. In particular, the space $C^0([0,T];X)$ is a Banach space when equipped with the norm

$$\|v(\cdot,\cdot)\|_{C^0([0,T];X)} \triangleq \max_{t\in[0,T]} \|v(\cdot,t)\|_X \,, \tag{6}$$

and space $C^l([0,T];X)$ is a Banach space when equipped with the norm

$$\|v(\cdot,\cdot)\|_{C^l([0,T];X)} \triangleq \max_{0\leq m\leq l} \left\| \frac{\partial^m v(\cdot,\cdot)}{\partial t^m} \right\|_{C^0([0,T];X)} . \tag{7}$$

In the following, given two Banach spaces X and Y, respectively, $\mathscr{L}(X;Y)$ denotes the space of (possibly unbounded) linear operators from X to Y, whereas $\mathscr{B}(X;Y)$ the space of bounded linear operators from X to Y, abbreviated $\mathscr{B}(X)$ whenever $Y = X$. For $l \in \mathbb{N}_0$, $C^l([0,T];\mathscr{L}(X;Y))$ and $C^l([0,T];\mathscr{B}(X;Y))$ denote the spaces of (possibly unbounded) and bounded linear operators from X to Y, respectively, whose coefficients are l times continuously differentiable on $[0,T]$. The group of operators on a Banach space X that are infinitesimal generators of a C_0-semigroup satisfying $\|T(t)\| \leq \mathrm{e}^{\omega t}$ is conventionally denoted by $\mathscr{G}(1,\omega)$ [41, 42].

Finally, $\mathbf{M}_{m\times n}(\mathbb{R})$, $\mathbf{Skew}_n(\mathbb{R})$, and $\mathbf{GL}_n(\mathbb{R})$ denote the groups of matrices, skew symmetric matrices, and invertible matrices, respectively, assuming values in $\mathbb{R}^{m\times n}$ and $\mathbb{R}^{n\times n}$; the identity matrix is denoted by $I_n \in \mathbf{GL}_n(\mathbb{R})$. $\mathbf{SO}_n(\mathbb{R})$ denotes the group of unitary rotations in $\mathbb{R}^n$.

With the above premises, existence and uniqueness properties for the hyperbolic equations encountered in rolling contact mechanics may be studied within the framework provided by the semigroup theory, after restating them in an abstract setting. In this paper, the focus is primarily on regular (*i.e.*, strict) solutions, which enjoy peculiar smoothness properties that are required for the error analysis performed in Section 4. In particular, considering a generic domain $\Omega \subset \mathbb{R}^d$ with boundary $\Gamma \triangleq \partial\Omega$, regular solutions are sought in the Hilbert space $L^2(\Omega;\mathbb{R}^n)$. Two separate classes of IBVPs are considered in what follows: equations in one space dimension, and equations in several space dimensions.

2.2. Problems in one space dimension

In this paper, the considered IBVPs involving a single space dimension generalise those derived in, *e.g.*, [32]. More specifically, by setting explicitly $\Omega = (0,1)$, the following structure is assumed:

$$\frac{\partial u(x,t)}{\partial t} + a(x,t)\frac{\partial u(x,t)}{\partial x} = B(t)u(x,t) + C(t)u(1,t) + f(x,t), \qquad \text{for } (x,t) \in (0,1)\times(0,T), \tag{8a}$$

$$u(0,t) = 0, \qquad \text{for } t \in (0,T), \tag{8b}$$

$$u(x,0) = u_0(x), \qquad \text{for } x \in (0,1), \tag{8c}$$

where $u(x,t) \in \mathbb{R}^n$ is the unknown solution, $a(x,t) \in \mathbb{R}$ denotes the transport velocity, $f(x,t) \in \mathbb{R}^n$ is the external forcing term, $C \in C^1([0,T];\mathbf{M}_{n\times n}(\mathbb{R}))$ and $B \in C^1([0,T];\mathscr{B}(L^2((0,1);\mathbb{R}^n)))$ is a bounded operator, typically having the form

$$(Bv)(x,t) = \tilde{B}(t)v(x) + \int_0^1 K(x,t)v(x)\,\mathrm{d}x, \tag{9}$$

with $\tilde{B} \in C^1([0,T];\mathbf{M}_{n\times n}(\mathbb{R}))$ and $K \in C^1([0,1]\times[0,T];\mathbf{M}_{n\times n}(\mathbb{R}))$.

The following Assumption 2.1 is supposed to hold concerning the considered IBVP in one space dimension, which facilitates the analysis.

Assumption 2.1. *The transport velocity satisfies* $a \in C^1([0,1]\times[0,T];[a_{\min},a_{\max}])$, *with* $a_{\min} > 0$.

Example 2.1 (Brush models on a time-varying domain)**.** After opportunely performing a change of variables, the brush models on a time-varying domain may be recast in the form of equation (8) with $u(x,t) \in \mathbb{R}^2$, $B(t) = 0$, and

$$a(x,t) \triangleq \frac{1}{2\alpha(t)}(1 + (1-2x)\dot{\alpha}(t)), \tag{10a}$$

$$C(t) \triangleq (1-\dot{\alpha}(t))(I_2 + 2\alpha(t)M)^{-1}M, \tag{10b}$$

$$f(x,t) \triangleq (I_2 + \alpha(t)M)^{-1}\sigma(t) + \alpha(t)\begin{bmatrix} 0 \\ 1-2x \end{bmatrix}\varphi(t), \tag{10c}$$

where $\alpha \in C^1([0,T];[\alpha_{\min},\alpha_{\max}])$ with $\alpha_{\min} > 0$, $\dot{\alpha} \in C^1([0,T];[\dot{\alpha}_{\min},\dot{\alpha}_{\max}])$, $\max\{|\dot{\alpha}_{\min}|,|\dot{\alpha}_{\max}|\} < 1$, $(\sigma,\varphi) \in C^1([0,T];\mathbb{R}^3)$, and $M \in \mathbf{GL}_2(\mathbb{R})$ is a positive definite, diagonal matrix [32]. Note that the assumptions on $\alpha(t)$ and $\dot{\alpha}(t)$ imply also that $C \in C^1([0,T];\mathbf{M}_{2\times 2}(\mathbb{R}))$.

The formulation presented in Example 2.1 has been recently introduced in [7] in the context of transient tyre modelling, limited to the case of a fixed contact patch ($\dot{\alpha}(t) = 0$ for all $t \in [0,T]$), and then further developed in [16,32]. Concerning applications in railway dynamics, the same PDEs have been obtained for a time-varying contact patch in [33], with $C(t) = 0$ for all $t \in [0,T]$. In both the automotive and railway fields, the variable $u(x,t) \in \mathbb{R}^2$ collects the tangential deformations of the material particles travelling inside the contact patch, relatively to the road or rail surface, respectively. The transport velocity $a(x,t) \in \mathbb{R}$, representing instead the rolling speed of the tyre or railway wheel, is clearly the same for all the components of $u(x,t)$.

Example 2.2 (LuGre-brush models on a time-varying domain)**.** After opportunely performing a change of variables, the LuGre-brush models with a spatially constant pressure distribution on a time-varying domain may be recast in the form of equation (8) with $u(x,t) \in \mathbb{R}^2$, $a(x,t)$ and $f(x,t)$ reading as in equations (10a) and (10c), respectively, and

$$C(t) \triangleq (1-\dot{\alpha}(t))(I_2 + 2\alpha(t)M_1M_2p(t))^{-1}M_1M_2p(t), \tag{11a}$$

$$\tilde{B}(t) \triangleq -\beta(t)M_1, \tag{11b}$$

$$K(x,t) \equiv K(t) \triangleq 2\alpha(t)(1-\dot{\alpha}(t))(I_2 + 2\alpha(t)M_1M_2p(t))^{-1}M_1M_2\left(\beta(t)M_1p(t) - \frac{\partial p(t)}{\partial t}\right), \tag{11c}$$

where $\alpha(t)$ and $\dot{\alpha}(t)$ satisfy the same assumptions as previously, $\beta \in C^1([0,T];\mathbb{R}_{\geq 0})$, $p \in C^1([0,T];[p_{\min},p_{\max}])$, with $p_{\min} > 0$, and M_1, $M_2 \in \mathbf{GL}_2(\mathbb{R})$ are positive definite diagonal matrices [32].

Also in the context of tyre dynamics, and limited to the case $\dot{\alpha}(t) = 0$ and $C(t) = 0$ for all $t \in [0,T]$, the LuGre-brush models were derived in [17–20] and studied extensively also in [21–23]. The first formulation accounting for the presence of boundary terms has recently appeared in [32]. According to such a model, $u(x,t) \in \mathbb{R}^2$ is interpreted either as a tangential deformation or as an internal frictional variable.

2.2.1. Well-posedness

The well-posedness of IBVPs of the same type as in equation (8) may be conveniently proved within the theoretical framework offered by the semigroup theory. In particular, considering for a moment the case $B(t) = 0$, the IBVP (8) simplifies to

$$\frac{\partial u(x,t)}{\partial t} + a(x,t)\frac{\partial u(x,t)}{\partial x} = C(t)u(1,t) + f(x,t), \qquad \text{for } (x,t) \in (0,1)\times(0,T), \tag{12a}$$

$$u(0,t) = 0, \qquad \text{for } t \in (0,T), \tag{12b}$$

$$u(x,0) = u_0(x), \qquad \text{for } x \in (0,1), \tag{12c}$$

which may be recast in abstract formulation as follows:

$$\frac{\mathrm{d}u(t)}{\mathrm{d}t} = A(t)u(t) + f(t), \qquad \text{for } t \in (0,T), \tag{13a}$$

$$u(0) = u_0, \tag{13b}$$

where, for each $t \in [0,T]$, the unbounded operator $(A(t), D(A(t)))$, $A(t) : D(A(t)) \mapsto L^2((0,1);\mathbb{R}^n)$, is assumed to be the infinitesimal generator of a C_0-semigroup on the Hilbert space $L^2((0,1);\mathbb{R}^n)$. In fact, owing to Assumption 2.1, the operator $(A(t), D(A(t)))$ may be defined as[1]

$$(Av)(x,t) \triangleq -a(x,t)\frac{\partial v(x)}{\partial x} + C(t)v(1), \tag{14a}$$

$$D(A(t)) \equiv D \triangleq \Big\{ v \in H^1((0,1);\mathbb{R}^n) \;\Big|\; v(0) = 0 \Big\}. \tag{14b}$$

Starting with the abstract formulation described by equations (13) and (14), the procedure to prove the well-posedness of the IBVP (12) relies on showing closedness and quasi-dissipativity properties for the operator $(A(t), D)$. In this context, Assumption 2.1 ensures the invertibility of the operator $(A(t), D)$, which is required in the next Lemma 2.1.

Lemma 2.1 (Closedness)**.** *Under Assumption 2.1, the operator $(A(t), D)$ as defined in equation (14) is closed.*

Proof. To prove that $(A(t), D)$ is closed, it suffices to show that, for all $t \in [0,T]$, there exists $\lambda \in \mathbb{R}_{>0}$ independent of t such that $A(t) - \lambda I$ is invertible, where, for brevity, $I = I_{L^2((0,1);\mathbb{R}^n)}$ (see, *e.g.*, [43], Thm. 4.2-C). By setting

$$((A - \lambda I)v)(x,t) = -a(x,t)\frac{\partial v(x)}{\partial x} - \lambda v(x) + C(t)v(1) = w(x), \tag{15}$$

it may be deduced that

$$v(x) = \int_0^x \frac{C(t)}{a(x',t)} \exp\!\left(-\int_{x'}^x \frac{\lambda}{a(\tilde{x},t)}\,\mathrm{d}\tilde{x}\right)\mathrm{d}x' v(1) - \int_0^x \frac{w(x')}{a(x',t)} \exp\!\left(-\int_{x'}^x \frac{\lambda}{a(\tilde{x},t)}\,\mathrm{d}\tilde{x}\right)\mathrm{d}x'. \tag{16}$$

Computing $v(1)$ in turn yields

$$\begin{aligned} v(x) = \Big((A - \lambda I)^{-1} w\Big)(x,t) = -\tilde{\Psi}(x,t) \int_0^1 \frac{w(x)}{a(x,t)} \exp\!\left(-\int_x^1 \frac{\lambda}{a(x',t)}\,\mathrm{d}x'\right)\mathrm{d}x \\ - \int_0^x \frac{w(x')}{a(x',t)} \exp\!\left(-\int_{x'}^x \frac{\lambda}{a(\tilde{x},t)}\,\mathrm{d}\tilde{x}\right)\mathrm{d}x', \end{aligned} \tag{17}$$

with

$$\tilde{\Psi}(x,t) \triangleq \int_0^x \frac{C(t)}{a(x',t)} \exp\!\left(-\int_{x'}^x \frac{\lambda}{a(\tilde{x},t)}\,\mathrm{d}\tilde{x}\right)\mathrm{d}x' \Psi^{-1}(t), \tag{18}$$

where, for all $t \in [0,T]$ and $a \in C^1([0,1]\times[0,1];[a_{\min}, a_{\max}])$ with $a_{\min} > 0$, the matrix

$$\Psi(t) \triangleq I_n - \int_0^1 \frac{C(t)}{a(x,t)} \exp\!\left(-\int_x^1 \frac{\lambda}{a(x',t)}\,\mathrm{d}x'\right)\mathrm{d}x, \tag{19}$$

is invertible for an appropriate choice of λ independent of t. In particular, since

$$\int_0^1 \frac{1}{a(x,t)} \exp\!\left(-\int_x^1 \frac{\lambda}{a(x',t)}\,\mathrm{d}x'\right)\mathrm{d}x \le \frac{a_{\max}}{\lambda a_{\min}}, \qquad \lambda \in \mathbb{R}_{>0}, \tag{20}$$

[1]For what follows, the time variable is often interpreted as a parameter $t \in [0,T]$ [40]. In this context, it is crucial to observe that, even though the operator $A(t)$ is time-dependent, its domain $D(A(t)) = D(A(0)) \equiv D$ is not, owing to Assumption 2.1. For this reason, the notation $(A(t), D(A(t)))$ is sometimes abbreviated as $(A(t), D)$.

choosing

$$\lambda > \frac{a_{\max}}{a_{\min}} \sup_{t\in[0,T]} \|C(t)\| \tag{21}$$

ensures $\Psi(t)$ in equation (19) to be invertible, *i.e.*, $\Psi \in C^1([0,T];\mathbf{GL}_n(\mathbb{R}))$. Since, according to equation (21) $\lambda \in \mathbb{R}_{>0}$, can be selected such that $(A(t)-\lambda I)^{-1}$ exists for all $t \in [0,T]$, $(A(t)-\lambda I, D)$ is closed, implying that $(A(t), D)$ is also closed. □

Proposition 2.1 (Adjoint operator)**.** *The adjoint operator* $(A^*(t), D(A^*(t)))$, $A^*(t) : D(A^*(t)) \mapsto L^2((0,1);\mathbb{R}^n)$ *of the operator* $(A(t), D)$ *defined in equation* (14) *is given by*

$$(A^*v)(x,t) = \frac{\partial}{\partial x}\left(a(x,t)v(x)\right), \tag{22a}$$

$$D(A^*(t)) = \left\{ v \in H^1((0,1);\mathbb{R}^n) \;\middle|\; v(1) = \frac{C^{\mathrm{T}}(t)}{a(1,t)} \int_0^1 v(x)\,\mathrm{d}x \right\}. \tag{22b}$$

Proof. Since there exists $\lambda \in \mathbb{R}_{>0}$ such that $(A(t)-\lambda I, D)$ admits a bounded inverse, it is sufficient to deduce an expression for the adjoint $(A(t)-\lambda I)^{-1^*} = (A(t)-\lambda I)^{*^{-1}}$ of $(A(t)-\lambda I)^{-1}$, and then exploit the fact that $(A(t)-\lambda I)^* = A^*(t) - \lambda I$ (see, *e.g.*, [45], Lem. A.3.72). Starting with equation (17), an application of Fubini's theorem yields

$$\begin{aligned}\Big((A-\lambda I)^{-1^*}v\Big)(x,t) = \Big((A-\lambda I)^{*^{-1}}v\Big)(x,t) = -\frac{1}{a(x,t)}\exp\!\left(-\int_x^1 \frac{\lambda}{a(x',t)}\,\mathrm{d}x'\right)\int_0^1 \tilde{\Psi}^{\mathrm{T}}(x,t)v(x)\,\mathrm{d}x \\ -\frac{1}{a(x,t)}\int_x^1 \exp\!\left(-\int_x^{x'} \frac{\lambda}{a(\tilde{x},t)}\,\mathrm{d}\tilde{x}\right)v(x')\,\mathrm{d}x'.\end{aligned} \tag{23}$$

Consider now the operator $((A(t)-\lambda I)^*, D((A(t)-\lambda I)^*))$, $(A(t)-\lambda I)^* : D((A(t)-\lambda I)^*) \mapsto L^2((0,1);\mathbb{R}^n)$ defined as

$$((A-\lambda I)^*v)(x,t) = \frac{\partial}{\partial x}\left(a(x,t)v(x)\right) - \lambda v(x), \tag{24a}$$

$$D((A(t)-\lambda I)^*) = \left\{ v \in H^1((0,1);\mathbb{R}^n) \;\middle|\; v(1) = \frac{C^{\mathrm{T}}(t)}{a(1,t)} \int_0^1 v(x)\,\mathrm{d}x \right\}. \tag{24b}$$

It may be verified that $(A(t)-\lambda I)^*(A(t)-\lambda I)^{-1^*} = I_{L^2((0,1);\mathbb{R}^n)}$ and $(A(t)-\lambda I)^{-1^*}(A(t)-\lambda I)^* = I_{D((A(t)-\lambda I)^*)}$, which then yields equation (22). □

Lemma 2.2 (Quasi-dissipativity)**.** *The operator* $(A(t), D)$ *defined according to equation* (14)*, together with its adjoint* $(A^*(t), D(A^*(t)))$*, is quasi-dissipative with constant* ω *given by*

$$\omega \triangleq \frac{1}{2}\left(\sup_{t\in[0,T]} \left\| \frac{\partial a(\cdot,t)}{\partial x} \right\|_\infty + \frac{\sup_{t\in[0,T]} \|C(t)\|^2}{\inf_{t\in[0,T]} a(1,t)} \right). \tag{25}$$

Proof. Considering the operator $(A(t), D)$, taking the inner product on $L^2((0,1);\mathbb{R}^n)$ and integrating by parts yields

$$\begin{aligned}\langle A(t)v, v\rangle_{L^2((0,1);\mathbb{R}^n)} &= -\int_0^1 a(x,t)\frac{\partial v^{\mathrm{T}}(x)}{\partial x}v(x)\,\mathrm{d}x + v^{\mathrm{T}}(1)C^{\mathrm{T}}(t)\int_0^1 v(x)\,\mathrm{d}x \\ &= -\frac{1}{2}\int_0^1 a(x,t)\frac{\partial}{\partial x}\|v(x)\|_2^2\,\mathrm{d}x + v^{\mathrm{T}}(1)C^{\mathrm{T}}(t)\int_0^1 v(x)\,\mathrm{d}x \\ &= -\frac{1}{2}a(1,t)\|v(1)\|_2^2 + \frac{1}{2}\int_0^1 \frac{\partial a(x,t)}{\partial x}\|v(x)\|_2^2\,\mathrm{d}x \\ &\quad + v^{\mathrm{T}}(1)C^{\mathrm{T}}(t)\int_0^1 v(x)\,\mathrm{d}x, \quad \text{for } v \in D.\end{aligned} \tag{26}$$

Applying Cauchy–Schwarz' and then the generalised form of Young's inequality for products to the last term on the right-hand side of equation (26) gives

$$\begin{aligned}\langle A(t)v, v\rangle_{L^2((0,1);\mathbb{R}^n)} \leq -\frac{1}{2}\left(\inf_{t\in[0,T]} a(1,t) - \frac{1}{\varepsilon}\sup_{t\in[0,T]}\|C(t)\|^2\right)\|v(1)\|_2^2 \\ + \frac{1}{2}\left(\sup_{t\in[0,T]}\left\|\frac{\partial a(\cdot,t)}{\partial x}\right\|_\infty + \varepsilon\right)\|v(\cdot)\|^2_{L^2((0,1);\mathbb{R}^n)}, \quad \text{for } v \in D.\end{aligned} \tag{27}$$

Therefore, selecting

$$\varepsilon \triangleq \frac{\sup_{t\in[0,T]}\|C(t)\|^2}{\inf_{t\in[0,T]} a(1,t)} \tag{28}$$

leads to $\langle A(t)v, v\rangle_{L^2((0,1);\mathbb{R}^n)} \leq \omega\|v(\cdot)\|^2_{L^2((0,1);\mathbb{R}^n)}$ with ω defined as in equation (25).

Additionally, starting with equation (22), similar manipulations as previously give

$$\begin{aligned}\langle A^*(t)v, v\rangle_{L^2((0,1);\mathbb{R}^n)} &= \int_0^1 \frac{\partial}{\partial x}\left(a(x,t)v^{\mathrm{T}}(x)\right)v(x)\,\mathrm{d}x \\ &= a(1,t)\|v(1)\|_2^2 - a(0,t)\|v(0)\|_2^2 - \int_0^1 a(x,t)v^{\mathrm{T}}(x)\frac{\partial v(x)}{\partial x}\,\mathrm{d}x \\ &= \frac{1}{2}a(1,t)\|v(1)\|_2^2 - \frac{1}{2}a(0,t)\|v(0)\|_2^2 \\ &\quad + \frac{1}{2}\int_0^1 \frac{\partial a(x,t)}{\partial x}\|v(x)\|_2^2\,\mathrm{d}x, \quad \text{for } v \in D(A^*(t)).\end{aligned} \tag{29}$$

Using the BC in equation (22b) and then applying the Cauchy–Schwarz' inequality yields

$$\begin{aligned}\langle A^*(t)v, v\rangle_{L^2((0,1);\mathbb{R}^n)} \leq \frac{1}{2}\left(\sup_{t\in[0,T]}\left\|\frac{\partial a(\cdot,t)}{\partial x}\right\|_\infty + \frac{\sup_{t\in[0,T]}\|C(t)\|^2}{\inf_{t\in[0,T]} a(1,t)}\right) \\ \times \|v(\cdot)\|_{L^2((0,1);\mathbb{R}^n)}, \quad \text{for } v \in D(A^*(t)).\end{aligned} \tag{30}$$

By combining equations (27) and (30), the result follows. □

The next theorem asserts the main well-posedness result for the IBVP (12).

Theorem 2.1 (Existence and uniqueness). *If Assumption 2.1 holds, for all* $f \in C^1([0,T];L^2((0,1);\mathbb{R}^n))$ *and* $u_0 \in D$, *the IBVP* (12) *admits a unique strict solution* $u \in C^1([0,T];L^2((0,1);\mathbb{R}^n)) \cap C^0([0,T];D)$ *given by*

$$u(t) = U_A(t,0)u_0 + \int_0^t U_A(t,t')f(t')\,\mathrm{d}t', \tag{31}$$

where $U_A(t,\tilde{t})$ *denotes the evolution operator associated with the infinitesimal generator* $(A(t),D)$.

Proof. Since $C_0^1([0,1];\mathbb{R}^n) \subset D(A(t)) \equiv D$, the operator $(A(t),D)$ as defined in equation (14) is dense, *i.e.*, $\overline{D} = L^2((0,1);\mathbb{R}^n)$. Moreover, it is closed and quasi-dissipative together with its adjoint $(A^*(t),D(A^*(t)))$ according to Lemmas 2.1 and 2.2. It follows from Lumer–Phillips' theorem (see, *e.g.*, [44], Cor. 2.2.3 or [45], Cor. 2.3.3) that, for $t \in [0,T]$, $A(t)$ is the infinitesimal generator of a C_0-semigroup. In particular, $A(t) \in \mathscr{G}(1,\omega)$, with ω as in equation (25). Therefore, the family $\{A(t)\}_{t\in[0,T]}$ is stable. Since $D(A(t)) = D(A(0)) \equiv D$ is independent of t and, for every $u_0 \in D$, $A(t)u_0$ is continuously differentiable in $L^2((0,1);\mathbb{R}^n)$ by Assumption 2.1, there exists unique strict solution $u \in C^1([0,T];L^2((0,1);\mathbb{R}^n)) \cap C^0([0,T];D)$ reading as in equation (31) for all $f \in C^1([0,T];L^2((0,1);\mathbb{R}^n))$ and $u_0 \in D$ (see [46], Thm. 4.5.4 or [47], 7.6). □

Concerning the complete formulation with $B(t) \neq 0$, Corollary 2.1 finally asserts the well-posedness of the IBVP (8).

Corollary 2.1 (Existence and uniqueness). *If Assumptions 2.1 holds, the IBVP* (8) *admits a unique strict solution* $u \in C^1([0,T];L^2((0,1);\mathbb{R}^n)) \cap C^0([0,T];D)$ *for all* $f \in C^1([0,T];L^2((0,1);\mathbb{R}^n))$ *and* $u_0 \in D$.

Proof. Consider again the operator $(A(t),D)$ as in equation (14) and define the operator $(\tilde{A}(t),D(\tilde{A}(t)))$, with $(\tilde{A}v)(x,t) = (Av)(x,t) + (Bv)(x,t)$ and $D(\tilde{A}(t)) = D(A(t)) = D(A(0)) \equiv D$ independent of t[2]. Since $A(t) \in \mathscr{G}(1,\omega)$ and $\|B(t)\| \leq B_{\max}$ for all $t \in [0,T]$, it follows that $\tilde{A}(t) \in \mathscr{G}(1,\omega + B_{\max})$, and consequently the family $\{\tilde{A}(t)\}_{t\in[0,T]}$ is stable ([47], Thm. 7.4 or [48], 5.2.3). Moreover, for every $u_0 \in D$, $\tilde{A}(t)u_0$ is continuously differentiable in $L^2((0,1);\mathbb{R}^n)$, which ensures the existence of a unique strict solution $u \in C^1([0,T];L^2((0,1);\mathbb{R}^n)) \cap C^0([0,T];D)$ for all $f \in C^1([0,T];L^2((0,1);\mathbb{R}^n))$ and $u_0 \in D$. □

Theorem 2.1 and Corollary 2.1 conclude the analysis of IBVPs in one space dimension.

2.3. System in several space dimensions

In the context of contact mechanics studies, transport equations in several space dimensions describe the dynamics of rolling and slipping bodies, including tyres, railway wheels, and elastic spheres [14,15,24].

More specifically, concerning systems in several space dimensions, the following structure for the IBVP is considered in this paper:

$$\frac{\partial u(x,t)}{\partial t} + (a(x,t)\cdot\nabla)u(x,t) = B(t)u(x,t) + f(x,t), \qquad \text{for } (x,t) \in \Omega \times (0,T), \tag{32a}$$

$$u(x,t) = 0, \qquad \text{for } (x,t) \in \Gamma_- \times (0,T), \tag{32b}$$

$$u(x,0) = u_0(x), \qquad \text{for } x \in \Omega, \tag{32c}$$

where $u(x,t) \in \mathbb{R}^n$, $a(x,t) \in \mathbb{R}^d$, $d \geq 2$, $f(x,t) \in \mathbb{R}^n$ is the external forcing term, $B \in C^1([0,T];\mathbf{M}_{n\times n}(\mathbb{R}))$, the open set $\Omega \subset \mathbb{R}^d$, represents the spatial domain and

$$\Gamma_+ = \big\{x \in \Gamma \;\big|\; a(x,t)\cdot\nu(x) > 0\big\}, \tag{33a}$$

$$\Gamma_0 = \big\{x \in \Gamma \;\big|\; a(x,t)\cdot\nu(x) = 0\big\}, \tag{33b}$$

[2]Here, $D(A(t)) = D(A(0)) \equiv D$ is considered a Banach space equipped with the graph norm $\|v(\cdot)\|_D^2 = \|v(\cdot)\|^2_{L^2((0,1);\mathbb{R}^n)} + \|\tilde{A}(0)v(\cdot)\|^2_{L^2((0,1);\mathbb{R}^n)}$.

$$\Gamma_- = \big\{ x \in \Gamma \;\big|\; a(x,t) \cdot \nu(x) < 0 \big\}, \tag{33c}$$

being $\nu(x) \in \mathbb{R}^d$ the outward unit normal to Γ. It should be observed that, unless the boundary Γ is sufficiently smooth, the outward unit normal $\nu(x)$ may not be defined for some points belonging to Γ. In the following, the set of such points is denoted by $\chi \subset \Gamma$.

The PDE (32a) describes a vector-valued transport equation whose scalar components are coupled *via* the matrix $B \in C^1([0,T]; \mathbf{M}_{n\times n}(\mathbb{R}))$. It is obvious that the matrix $B(t)$ is the infinitesimal generator of a C_0-semigroup[3], with solution operator denoted by $U_B(t,\tilde{t})$. Therefore, substituting $u(x,t) \triangleq U_B(t,0)w(x,t)$ into equation (32a) yields

$$U_B(t,0)\left(\frac{\partial w(x,t)}{\partial t} + (a(x,t)\cdot\nabla)w(x,t)\right) = -\left(\frac{\partial U_B(t,0)}{\partial t} - B(t)U_B(t,0)\right)w(x,t) + f(x,t), \quad \text{for } (x,t) \in \Omega \times (0,T). \tag{34}$$

Since $U_B(0,0) = I_n$, the following matrix ODE is identically satisfied:

$$\frac{\partial U_B(t,0)}{\partial t} = B(t)U_B(t,0), \qquad \text{for } t \in [0,T]. \tag{35}$$

Additionally, by observing that the solution operator is invertible, *i.e.*, $C^1([0,T]; \mathbf{GL}_n(\mathbb{R})) \ni U_B^{-1}(t,0) \equiv U_B(0,t)$ exists for every $t \in [0,T]$, the original system described by equation (32) may be recast in the following equivalent form:

$$\frac{\partial w(x,t)}{\partial t} + (a(x,t)\cdot\nabla)w(x,t) = g(x,t), \qquad \text{for } (x,t) \in \Omega \times (0,T), \tag{36a}$$

$$w(x,t) = 0, \qquad \text{for } (x,t) \in \Gamma_- \times (0,T), \tag{36b}$$

$$w(x,0) = w_0(x) = u_0(x), \qquad \text{for } x \in \Omega, \tag{36c}$$

being $g(x,t) \triangleq U_B(0,t)f(x,t)$. The technique outlined above may be conveniently applied to the rolling contact problems considered, *e.g.*, in [14,15], which are or may be recast[4] in the same form as that described by equation (32).

Concerning the study of the IBVPs (32) and (36), a common problem is that, when the velocity field $a(x,t)$ is time-dependent, the sets defined according to equation (33) may also vary over time, that is, $\Gamma_+ = \Gamma_+(t)$, $\Gamma_0 = \Gamma_0(t)$ and $\Gamma_- = \Gamma_-(t)$. Moreover, the product $a(x,t)\cdot\nu(x)$ vanishes for all the points of the boundary belonging to Γ_- (characteristic condition). As opposed to the one-dimensional case, for general domains $\Omega \subset \mathbb{R}^d$, there is no simple characterisation guaranteeing that the sets in equation (33) are time-independent, whilst also ensuring that the noncharacteristic condition is never violated on the boundary (see, *e.g.*, the discussions reported in [50–52]). Therefore, mainly for the purpose of coherence, a simplified version of the IBVP (36), where the vector field $a(x,t) = a(x)$ is assumed to be time-independent, is considered in the following. Returning to the standard notation for a matter of convenience, the corresponding IBVP is stated as

$$\frac{\partial u(x,t)}{\partial t} + (a(x)\cdot\nabla)u(x,t) = f(x,t), \qquad \text{for } (x,t) \in \Omega \times (0,T), \tag{37a}$$

$$u(x,t) = 0, \qquad \text{for } (x,t) \in \Gamma_- \times (0,T), \tag{37b}$$

$$u(x,0) = u_0(x), \qquad \text{for } x \in \Omega. \tag{37c}$$

A typical problem of the form (32) encountered in rolling contact mechanics is described in Example 2.3 below.

[3]This obviously remains true if $B \in C^0([0,T]; \mathbf{M}_{n\times n}(\mathbb{R}))$.

[4]For example, IBVPs evolving on time-varying domains, such as those considered in [14, 15], may be restated according to equation (32).

Example 2.3. Hyperbolic systems in two space dimensions govern the equations of the brush and LuGre-brush models on fixed domains. In particular, when accounting for large spin slips, both formulations are in the form of equation (32), with $u(x,t) \in \mathbb{R}^2$, $\Omega \subset \mathbb{R}^2$, and

$$a(x,t) \equiv a(x) = \begin{bmatrix} -\varepsilon_1 + \gamma x_2 \\ \varepsilon_2 - \gamma x_1 \end{bmatrix}, \tag{38a}$$

$$B(t) \equiv B = \begin{bmatrix} -\kappa_1 & -\psi \\ \psi & -\kappa_2 \end{bmatrix}, \tag{38b}$$

$$f(x,t) \equiv f(x) = \sigma + \begin{bmatrix} -\varphi x_2 \\ \varphi x_1 \end{bmatrix}, \tag{38c}$$

where $\kappa_1 = \kappa_2 = 0$ identically for the standard brush model and κ_1, $\kappa_2 \geq 0$ for the LuGre-brush models. For $B(t)$ constant, or commuting with its integral in the time-varying case, the corresponding evolution operator introduced in Section 2.3 reads evidently $U_B(t,\tilde{t}) = \exp(\int_{\tilde{t}}^{t} B(t')\,\mathrm{d}t')$. Concerning the standard brush models, the matrix $B(t)$ does not only commute even in the time-varying case, but it is also skew-symmetric, *i.e.*, $B(t) \in \mathbf{Skew}_2(\mathbb{R})$, and therefore the evolution operator is unitary ($\kappa_1 = \kappa_2 = 0$ implies more specifically $U_B(t,\tilde{t}) \in \mathbf{SO}_2(\mathbb{R})$). The problem may, in principle, be solved analytically using the method of the characteristic lines even when $B = B(t)$ and $f(x) = f(x,t)$ are time-varying. This may be accomplished either directly or by converting the original IBVP (32) into the equivalent one (37). Analytical solutions are reported, for example, in [14, 15, 24] concerning rectangular, circular, and elliptical domains.

The motivation for considering the simplified IBVP (37) resides in that the semigroup theory may be more easily applied, since the sets defined in equation (33) do not depend on time.

2.3.1. Well-posedness

The well-posedness of the IBVP (37) follows from a classical result obtained by Bardos [49], which provides the following abstract representation:

$$\frac{\mathrm{d}u(t)}{\mathrm{d}t} = Au(t) + f(t), \qquad \text{for } t \in (0,T), \tag{39a}$$

$$u(0) = u_0, \tag{39b}$$

where the unbounded operator $(A, D(A))$, $A : D(A) \mapsto L^2(\Omega;\mathbb{R}^n)$, is defined as

$$(Av)(x) \triangleq -(a(x)\cdot\nabla)v(x), \tag{40a}$$

$$D(A) \equiv D \triangleq \left\{ v \in L^2(\Omega;\mathbb{R}^n) \;\middle|\; (a\cdot\nabla)v \in L^2(\Omega;\mathbb{R}^n), \text{ and } v|_{\Gamma_-} = 0 \right\}. \tag{40b}$$

Theorem 2.2 asserts the well-posedness for the equivalent IBVP (37), and consequently also for the original formulation (32).

Theorem 2.2 (Existence and uniqueness [49])**.** *Assume that the field $A = a(x)\cdot\nabla$ can be extended to a field $\bar{A} = \bar{a}(x)\cdot\nabla$ defined on an open set $\Omega^* \subset \mathbb{R}^d$ such that $\overline{\Omega} \subset \Omega^*$, with $\bar{a} \in C^1(\Omega^*;\mathbb{R}^d)$ bounded on Ω^* together with its derivatives. Moreover, suppose that the boundary Γ of the domain Ω is piecewise C^1. Then, the IBVP (37) admits a unique strict solution $u \in C^1([0,T];L^2(\Omega;\mathbb{R}^n)) \cap C^0([0,T];D)$ for all $f \in C^1([0,T];L^2(\Omega;\mathbb{R}^n))$ and $u_0 \in D$.*

Sketch of the proof. Since, owing to the Theorem's assumptions, the trajectories of A intersecting $\Gamma_0 \cup \chi$ have zero measure, it can be shown that A is the infinitesimal generator of a C_0-semigroup (see [49]). In particular, $A \in \mathscr{G}(1,\omega)$, with $\omega \triangleq \frac{1}{2}\|\nabla\cdot a(\cdot)\|_\infty$. Therefore, for every $f \in C^1([0,T];L^2(\Omega;\mathbb{R}^n))$ and $u_0 \in D$, the IBVP (37) has a unique strict solution. □

Before concluding the analysis, it is perhaps worth mentioning that the extension of Theorem 2.2 to more general IBVPs, accounting for, *e.g.*, integral terms, may be worked out again within the mathematical framework provided by the perturbation theory of linear unbounded operators. A final consideration is formalised in Remark 2.1 below.

Remark 2.1 (Discussion about less regular solutions)**.** According to the abstract representation provided by equation (39), the solution to the IBVP (37) is formally given by a similar expression to that in equation (31). Concerning hyperbolic equations both in one and several space dimensions (Eqs. (8) and (37), respectively), it is worth observing that equation (31) has meaning even if $u_0 \in L^2(\Omega;\mathbb{R}^n)$ and $f \in L^p((0,T);L^2(\Omega;\mathbb{R}^n))$, $p \geq 1$. In such a case, the function in equation (31) is said to be a mild solution. Regarding systems in several space dimensions, the well-posedness asserted by Theorem 2.2 is limited to the case of a time-independent vector field $a(x,t) = a(x)$. However, in a very general setting, when, *e.g.*, $B \in C^0([0,T];\mathbf{M}_{n\times n}(\mathbb{R}^n))$, existence and uniqueness for the IBVP (32) may be established as in [53], considering the equivalent system (36).

3. Space semi-discretisation: discontinuous Galerkin finite element methods (DGMs)

The present section illustrates the main concepts and assumptions that are required to construct finite-dimensional approximations of hyperbolic evolution equations within the (DGM) framework. The proposed method relies on the spatial discretisation of the considered domain Ω, using a mesh and choosing an appropriate local polynomial behaviour within each mesh element. More specifically, in the remainder of this Section, the following hyperbolic IBVP is considered, which generalises those examined in Section 2:

$$\frac{\partial u(x,t)}{\partial t} + (a(x,t)\cdot\nabla)u(x,t) = B(t)u(x,t) + C(t)\int_\Gamma u(x,t)\,\mathrm{d}s + f(x,t), \qquad \text{for } (x,t)\in\Omega\times(0,T), \tag{41a}$$

$$u(x,t) = 0, \qquad \text{for } (x,t)\in\Gamma_-\times(0,T), \tag{41b}$$

$$u(x,0) = u_0(x), \qquad \text{for } x\in\Omega, \tag{41c}$$

with the data $a(x,t)\in\mathbb{R}^d$, $f(x,t)\in\mathbb{R}^n$, $B(t)\in\mathscr{B}(L^2(\Omega;\mathbb{R}^n))$, and $C(t)\in\mathbf{M}_{n\times n}(\mathbb{R})$ assumed to be sufficiently regular for what follows. In particular, specifying the term $B(t)=0$ for simplicity[5] and consistency of notation with Section 2, and assuming $\Gamma_-(t)=\Gamma_-$ to be constant over time, the above hyperbolic IBVP may be recast in abstract form by setting

$$(Av)(x,t) \triangleq -(a(x,t)\cdot\nabla)v(x) + C(t)\int_\Gamma v(x)\,\mathrm{d}s, \tag{42a}$$

$$D(A(t)) \triangleq \Big\{ v\in L^2(\Omega;\mathbb{R}^n) \;\Big|\; A(t)v\in L^2(\Omega;\mathbb{R}^n), \text{ and } v|_{\Gamma_-}=0 \Big\}, \tag{42b}$$

where it shall be supposed that $D(A(t)) = D(A(0))$. Such a condition is formalised according to the following Assumption 3.1, and is complemented with additional requirements imposed on the domain Ω and on matrix $C(t)\in\mathbf{M}_{n\times n}(\mathbb{R})$.

Assumption 3.1. *The following conditions are supposed to hold:*

(1) *The domain $D(A(t)) = D(A(0)) \equiv D$ is independent of the time.*
(2) *The domain Ω is bounded with compact boundary Γ.*
(3) *The matrix $C(t)\in\mathbf{M}_{n\times n}(\mathbb{R}) = 0$ whenever the condition $a(x,t)\cdot\nu(x)=0$ is satisfied for some $x\in\Gamma$.*

[5] As in Section 2, when the operator $B(t)$ is explicitly considered, the problem becomes equivalent by replacing $(A(t), D(A(t)))$ with $(\tilde{A}(t), D(\tilde{A}(t)))$, being $(\tilde{A}v)(x,t) \triangleq (Av)(x,t) + (Bv)(x,t)$ and $D(\tilde{A}(t)) = D(A(t))$.

Concerning the characterisation of the the domain $D(A(t)) \equiv D$, it is worth emphasising that all the IBVPs analysed in Section 2 may be recast in the form (13) with $(A(t), D(A(t)))$ according to equation (42). In particular, with reference to the one-dimensional problems investigated in Section 2.2, it is clear that Assumptions 2.1 and 3.1 render the definition of the domain $D(A(t)) \equiv D$ in equation (14) equivalent to that in equation (42).

Finally, the exact solution to the IBVP (13), with $(A(t), D(A(t)))$ defined as in equation (42), is supposed to satisfy at least $u \in C^0([0,T]; H^1(\Omega;\mathbb{R}^n))$. In the following, the notation is always abbreviated as $(A(t), D)$.

3.1. Space semi-discretisation of linear hyperbolic IBVPs

The continuous IBVP described by equation (13), with $(A(t), D)$ defined as in equation (42), may be approximated using functions $u_h(t) \in V_h$, being V_h a finite-dimensional space to be opportunely selected, by replacing the operator $(A(t), D)$ with its discrete counterpart $(A_h(t), V_{h\star})$, where $V_{h\star} \triangleq H^1(\Omega;\mathbb{R}^n) + V_h$ needs to be defined accordingly.

In particular, the functional spaces V_h considered in this paper are supposed to coincide with the broken polynomial spaces $\mathbb{P}^k_d(\mathcal{T}_h;\mathbb{R}^n)$, *i.e.*, $V_h \triangleq \mathbb{P}^k_d(\mathcal{T}_h;\mathbb{R}^n)$, defined with polynomial degree $k \in \mathbb{N}_0$ and with $\mathcal{T}_h$ being a mesh of elements T with faces F, and belonging to an admissible mesh sequence $\mathcal{T}_\mathcal{H} = \{\mathcal{T}_h\}_{h\in\mathcal{H}}$ with diameter $h \triangleq \max_{T\in\mathcal{T}_h} h_T$. In the following, the set of mesh faces $\mathcal{F}_h = \mathcal{F}_h^{\mathrm{i}} + \mathcal{F}_h^{\mathrm{b}}$ is also decomposed into the sets of interfaces $\mathcal{F}_h^{\mathrm{i}}$ and boundary faces $\mathcal{F}_h^{\mathrm{b}}$. The unit normals to ∂T and F, defined almost everywhere, are indicated with $\nu_{\partial T}(x)$ and $\nu_F(x)$. More specifically, considering two adjacent mesh elements $T_1, T_2 \in \mathcal{T}_h$, $\nu_F(x)$ is defined as $\nu_{\partial T_1}(x)$, that is, the unit normal to F at x pointing from T_1 to T_2 if $F \in \mathcal{F}_h^{\mathrm{i}}$, with $F = \partial T_1 \cap \partial T_2$; on the other hand, $\nu_F(x)$ coincides with $\nu(x)$, the outward unit normal to Γ at x, if $F \in \mathcal{F}_h^{\mathrm{b}}$.

For $v(x) \in \mathbb{R}$ defined on Ω, and smooth enough to admit, on all $F \in \mathcal{F}_h^{\mathrm{i}}$, a possibly two-valued trace, the *average* and *jump* are defined respectively as

$$\{\!\{v(x)\}\!\} \triangleq \frac{1}{2}\big(v(x)|_{T_1} + v(x)|_{T_2}\big), \tag{43a}$$

$$[\![v(x)]\!] \triangleq v(x)|_{T_1} - v(x)|_{T_2}\,. \tag{43b}$$

For vector-valued functions $v(x) \in \mathbb{R}^n$, averages and jumps are defined component-wise.

Finally, considering a real number $y \in \mathbb{R}$, its positive and negative parts $y^\oplus$, $y^\ominus \in \mathbb{R}_{\geq 0}$ are also defined for convenience as

$$y^\oplus \triangleq \frac{1}{2}(|y| + y), \tag{44a}$$

$$y^\ominus \triangleq \frac{1}{2}(|y| - y). \tag{44b}$$

Moreover, to alleviate the notation, inequalities of the type $a \leq Cb$, where C is a constant independent of h and the problem data, are often abbreviated as $a \lesssim b$ in what follows.

The next Section 3.1.1 recollects some useful polynomial approximation properties that are needed for the analyses conducted in Sections 3.2 and 4.3. Moreover, Sections 3.1.2 and 3.1.3 introduce some important assumptions and norms required for the characterisation of the discrete operator $(A_h(t), V_{h\star})$.

3.1.1. Polynomial approximation properties

Consider the L^2-orthogonal projection $\pi_h : L^2(\Omega;\mathbb{R}^n) \mapsto \mathbb{P}^k_d(\mathcal{T}_h;\mathbb{R}^n)$ onto the broken polynomial space $\mathbb{P}^k_d(\mathcal{T}_h;\mathbb{R}^n)$. The following polynomial approximation properties, formalised in Lemmas 3.1 and 3.2, are propaedeutic to the results advocated in Sections 3.2 and 4.3.

Lemma 3.1 (Optimality of L^2-orthogonal projection)**.** *Let $\mathcal{T}_\mathcal{H}$ be an admissible mesh sequence. Let $\pi_h : L^2(\Omega;\mathbb{R}^n) \mapsto \mathbb{P}^k_d(\mathcal{T}_h;\mathbb{R}^n)$ be the L^2-orthogonal projection onto $\mathbb{P}^k_d(\mathcal{T}_h;\mathbb{R}^n)$. Then, for all $s \in \{0,\dots,k+1\}$ and all $m \in \{0,\dots,s\}$, it holds that*

$$|v(\cdot) - \pi_h v(\cdot)|_{H^m(T;\mathbb{R}^n)} \leq C'_{\mathrm{p}} h_T^{s-m} |v(\cdot)|_{H^s(T;\mathbb{R}^n)}, \qquad \text{for } v \in H^s(T;\mathbb{R}^n), \tag{45}$$

where C'_{p} is independent of both T and h.

Proof. See Lemma 1.58 in [38]. □

Lemma 3.2 (Polynomial approximation on mesh faces)**.** *Under the same hypotheses of Lemma 3.1, assume additionally that $s \geq 1$. Then, for all $h \in \mathcal{H}$, all $T \in \mathcal{T}_h$, and all $F \in \mathcal{F}_T \triangleq \{F \in \mathcal{F}_h \mid F \subset \partial T\}$, the following inequalities hold:*

$$\|v(\cdot) - \pi_h v(\cdot)\|_{L^2(F;\mathbb{R}^n)} \leq C''_{\mathrm{p}} h_T^{s-1/2} |v(\cdot)|_{H^s(T;\mathbb{R}^n)}, \qquad \text{for } s \geq 1, \tag{46a}$$

$$\sum_{i=1}^{n} \left\| \nabla \left(v_i(\cdot) - \pi_h v_i(\cdot) \right)\big|_T \cdot \nu_{\partial T}(\cdot) \right\|_{L^2(F)} \leq C'''_{\mathrm{p}} h_T^{s-3/2} |v(\cdot)|_{H^s(T;\mathbb{R}^n)}, \qquad \text{for } s \geq 2, \tag{46b}$$

where C''_{p} and C'''_{p} are independent of both T and h.

Proof. The result is a direct consequence of the continuous trace inequality. □

3.1.2. Assumptions on the mesh

As already mentioned, in this paper, by setting $V_h \triangleq \mathbb{P}_d^k(\mathcal{T}_h;\mathbb{R}^n)$, space semi-discretisation is achieved using an upwind DGM, which is particularly suited to treat hyperbolic IBVPs. In particular, quasi-uniform mesh sequences are considered for simplicity, which essentially means that, for all $h \in \mathcal{H}$, $\max_{T\in\mathcal{T}_h} h_T \leq C \min_{T\in\mathcal{T}_h} h_T$.

Moreover, the following reference quantities are introduced:

$$\frac{1}{t_{\mathrm{c}}} \triangleq \max\left\{ \sup_{t\in[0,T]} \|\nabla \cdot a(\cdot,t)\|_\infty, \varepsilon_h \right\}, \quad \text{and} \quad \eta_{\mathrm{c}} \triangleq \sup_{t\in[0,T]} \|a(\cdot,t)\|_\infty, \tag{47a}$$

with $\varepsilon_h \in \mathbb{R}_{\geq 0}$ satisfying

$$\varepsilon_h \triangleq \begin{cases} 2\psi_h \frac{\sup_{t\in[0,T]} \|C(t)\|^2}{\inf_{(x,t)\in\Gamma\times[0,T]} |a(x,t)\cdot\nu(x)|}, & \text{if } \inf_{(x,t)\in\Gamma\times[0,T]} |a(x,t)\cdot\nu(x)| \in \mathbb{R}_{>0}, \\ 0, & \text{otherwise,} \end{cases} \tag{48}$$

for some $\psi_h > 1$. From the definitions above, it may be realised that η_{c} scales as a velocity, whereas t_{c} scales as the reciprocal of a time only if $\varepsilon_h = 0$. The inconsistency is due to the fact that the term ε_h arises from the cross product between a boundary term and an integral over the physical domain. Moreover, whenever $1/t_{\mathrm{c}} = 0$, $t_{\mathrm{c}} = \infty$, which corresponds to the case of constant advection velocity, no reaction, and absence of boundary terms ($C(t) = 0$ by assumption). Another time scale, defined more specifically as

$$t_\star \triangleq \min\{T, t_{\mathrm{c}}\}, \tag{49}$$

is also introduced for what follows. It is essential to clarify that, in the subsequent analyses, expressions involving $1/t_{\mathrm{c}}$ are conventionally evaluated at zero whenever $t_{\mathrm{c}} = \infty$. Moreover, according to equation (49), the following Assumption 3.2 is supposed to hold.

Assumption 3.2 (Assumption on the meshsize)**.** *The meshsize h is chosen such as to verify*

$$h \leq \eta_{\mathrm{c}} t_\star. \tag{50}$$

Assumption 3.2 prevents the local Damkhler number from being too large, and allows the meshsize to resolve the spatial variations of the transport velocity [38]. Moreover, such choice of h implies that a particle advected at speed η_{c} crosses at least one mesh element over the finite time interval $(0, T)$.

3.1.3. Norms and seminorms

Inspired by [38], the following seminorms on $V_{h\star} \triangleq H^1(\Omega;\mathbb{R}^n) + V_h$ are introduced, which are needed for the analysis conducted in Sections 3.2 and 3.3:

$$|v(\cdot)|_\eta^2 \triangleq \frac{1}{2}\int_\Gamma |a(x,t)\cdot\nu(x)|\,\|v(x)\|_2^2\,\mathrm{d}s + \frac{1}{2}\sum_{F\in\mathcal{F}_h^{\mathrm{i}}}\int_F |a(x,t)\cdot\nu_F(x)|\,\|[\![v(x)]\!]\|_2^2\,\mathrm{d}s, \tag{51a}$$

$$|v(\cdot)|_C^2 \triangleq \frac{1}{2}\,\|C(t)\|^2\,\|v(\cdot)\|_{L^2(\Gamma;\mathbb{R}^n)}^2\,, \tag{51b}$$

$$|v(\cdot)|_{\varepsilon_h}^2 \triangleq \begin{cases} |v(\cdot)|_\eta^2 - \frac{1}{\varepsilon_h}\,|v(\cdot)|_C^2\,, & \text{if } \varepsilon_h \in \mathbb{R}_{>0},\\ |v(\cdot)|_\eta^2 & \text{otherwise,}\end{cases} \tag{51c}$$

$$|v(\cdot)|_{\frac{\varepsilon_h}{2}}^2 \triangleq \begin{cases} |v(\cdot)|_{\varepsilon_h}^2 - \frac{1}{\varepsilon_h}\,|v(\cdot)|_C^2\,, & \text{if } \varepsilon_h \in \mathbb{R}_{>0},\\ |v(\cdot)|_\eta^2 & \text{otherwise.}\end{cases} \tag{51d}$$

It is worth clarifying, in particular, that the term $C(t)$ in equation (51b) represents the matrix of coefficients appearing in the IBVP (41), and hence the quantities defined according to equations (51c) and (51d) are actually seminorms, owing to an appropriate choice of the parameter ε_h satisfying equation (48) with $\psi_h > 1$. Accordingly, the following norms, similar to those considered in [38], are also defined on $V_{h\star}$:

$$\|v(\cdot)\|_h^2 \triangleq \frac{1}{t_{\mathrm{c}}}\,\|v(\cdot)\|_{L^2(\Omega;\mathbb{R}^n)}^2 + |v(\cdot)|_\eta^2\,, \tag{52a}$$

$$\|v(\cdot)\|_{h\star}^2 \triangleq \|v(\cdot)\|_h^2 + \sum_{T\in\mathcal{T}_h}\eta_{\mathrm{c}}\,\|v(\cdot)\|_{L^2(\partial T;\mathbb{R}^n)}^2\,. \tag{52b}$$

3.2. The discrete operator $(A_h(t), V_{h\star})$

The first step in anchieving space semi-discretisation consists in replacing the operator $(A(t), D)$ appearing in equations (13) and (42) with its discrete counterpart. In this paper, based predominantly on [38], a discrete operator with upwind regularisation is proposed. More specifically, the discrete operator $(A_h(t), V_{h\star})$, $A_h(t) : V_{h\star} \mapsto V_h$, is introduced as

$$\begin{aligned}\langle A_h(t)v, w_h\rangle_{L^2(\Omega;\mathbb{R}^n)} \triangleq &-\int_\Omega \Big[(a(x,t)\cdot\nabla_h)v(x)\Big]^{\mathrm{T}} w_h(x)\,\mathrm{d}x + \int_\Gamma v^{\mathrm{T}}(x)C^{\mathrm{T}}(t)\,\mathrm{d}s\int_\Omega w_h(x)\,\mathrm{d}x\\ &-\int_\Gamma (a(x,t)\cdot\nu(x))^{\ominus} v^{\mathrm{T}}(x)w_h(x)\,\mathrm{d}s\\ &+\sum_{F\in\mathcal{F}_h^{\mathrm{i}}}\int_F a(x,t)\cdot\nu_F(x)[\![v(x)]\!]^{\mathrm{T}}\{\!\{w_h(x)\}\!\}\,\mathrm{d}s\\ &-\frac{1}{2}\sum_{F\in\mathcal{F}_h^{\mathrm{i}}}\int_F |a(x,t)\cdot\nu_F(x)|\,[\![v(x)]\!]^{\mathrm{T}}[\![w_h(x)]\!]\,\mathrm{d}s, \quad \text{for } (v,w_h)\in V_{h\star}\times V_h,\end{aligned} \tag{53}$$

where the broken gradient $\nabla_h : H^1(\mathcal{T}_h) \mapsto L^2(\Omega;\mathbb{R}^d)$ is defined such that, for all $T \in \mathcal{T}_h$ and $v \in H^1(\mathcal{T}_h)$, $\nabla_h v(x)|_T \triangleq \nabla(v(x)|_T)$. In this context, it is also worth observing that the broken gradient coincides with the distributional one in $H^1(\Omega)$, and moreover, $v \in H^1(\Omega;\mathbb{R}^n)$ implies that $[\![v(x)]\!] = 0$ for all $F \in \mathcal{F}_h^{\mathrm{i}}$.

In this way, $(A_h(t), V_{h\star})$ may be used to formulate the equivalent space semi-discrete problem of the IBVP (13) as

$$\frac{\mathrm{d}u_h(t)}{\mathrm{d}t} = A_h(t)u_h(t) + f_h(t), \qquad \text{for } t\in(0,T), \tag{54a}$$

$$u_h(0) = \pi_h u_0, \tag{54b}$$
$$f_h(t) = \pi_h f(t), \qquad \text{for } t \in (0,T), \tag{54c}$$

where $\pi_h : L^2(\Omega;\mathbb{R}^n) \mapsto V_h$ denotes once again the L^2-projection onto $V_h \triangleq \mathbb{P}^k_d(\mathcal{T}_h;\mathbb{R}^n)$. By choosing a suitable basis for the space V_h, the semi-discrete IBVP (54) may be transformed into a system of linear ODEs for the time-varying components $u_h(t)$ on the selected basis [38].

Remark 3.1. In defining $(A_h(t), V_{h\star})$ according to equation (53), it has been assumed that $B(t) = 0$ for simplicity. The extension to the case where $B(t)$ is not identically zero is trivial. It is also worth clarifying that the following analyses are not affected by such a simplification, and the definition of the seminorms and norms as in equations (51) and (52) can easily accommodate the more general case, by simply modifying the quantities appearing in equation (47). On this matter, see also [38].

3.2.1. Characterisation of the discrete operator $(A_h(t), V_{h\star})$

Some technical results are preliminary needed to establish the stability and convergence of the proposed DGMs. In particular, the first result advocated here, formalised in Lemma 3.3, delivers a stronger version of the consistency property considered in [38], which accounts for time-shifting, whereas quasi-dissipativity properties for the operator $(A_h(t), V_{h\star})$ are asserted by Lemma 3.4.

Lemma 3.3 (Time-shifted consistency)**.** *Under Assumption 3.1, the discrete operator* $(A_h(t), V_{h\star})$ *is* time-shifted consistent*. That is, for any exact solution* $u \in C^1([0,T];L^2(\Omega;\mathbb{R}^n)) \cap C^0([0,T];H^1(\Omega;\mathbb{R}^n))$ *to the IBVP described by equations* (13) *and* (42)*, and* $w_h \in V_h$*, it satisfies*

$$\langle A_h(t)u(t'), w_h\rangle_{L^2(\Omega;\mathbb{R}^n)} = \langle A(t)u(t'), w_h\rangle_{L^2(\Omega;\mathbb{R}^n)}, \qquad \text{for } (t,t') \in [0,T]^2, \tag{55a}$$
$$\langle A_h(t)u(t'), w_h\rangle_{L^2(\Omega;\mathbb{R}^n)} = \langle \pi_h A(t)u(t'), w_h\rangle_{L^2(\Omega;\mathbb{R}^n)}, \qquad \text{for } (t,t') \in [0,T]^2. \tag{55b}$$

Proof. Since it solves the IBVP described by equations (13) and (42), $u \in C^0([0,T];H^1(\Omega;\mathbb{R}^n)) \cap C^0([0,T];D)$ by assumption. Moreover, since $D(A(t)) = D(A(0)) \equiv D$ is constant over time, the third term on the right-hand side of equation (53) vanishes for all $(t,t') \in [0,T]^2$, whereas $u \in C^0([0,T];H^1(\Omega;\mathbb{R}^n))$ implies $[\![u(x,t')]\!] = 0$ for all $F \in \mathcal{F}^{\mathrm{i}}_h$. Hence, equation (53) simplifies to

$$\begin{aligned}\langle A_h(t)u(t'), w_h\rangle_{L^2(\Omega;\mathbb{R}^n)} &= -\int_\Omega [(a(x,t)\cdot\nabla)u(x,t')]^{\mathrm{T}} w_h(x)\,\mathrm{d}x + \int_\Gamma u^{\mathrm{T}}(x,t')C^{\mathrm{T}}(t)\,\mathrm{d}s \int_\Omega w_h(x)\,\mathrm{d}x \\ &= \langle A(t)u(t'), w_h\rangle_{L^2(\Omega;\mathbb{R}^n)},\end{aligned} \tag{56}$$

therefore proving equation (55a). Moreover, recalling the definition of $\pi_h : L^2(\Omega;\mathbb{R}^n) \mapsto V_h$ provides

$$\langle \pi_h A(t)u(t'), w_h\rangle_{L^2(\Omega;\mathbb{R}^n)} = \langle A(t)u(t'), w_h\rangle_{L^2(\Omega;\mathbb{R}^n)}, \tag{57}$$

which, combined with the above equation (56), gives (55b). □

Lemma 3.3 generalises the classic notion of consistency ([38], Lem. 3.4).

Lemma 3.4 (Discrete quasi-dissipativity)**.** *For all* $v_h \in V_h$*, the operator* $(A_h(t), V_{h\star})$ *is quasi-dissipative with constant*

$$\omega_h \triangleq \frac{1}{2}\left(\sup_{t\in[0,T]} \|\nabla\cdot a(\cdot,t)\|_\infty + \varepsilon_h\right), \tag{58}$$

where ε_h *may be chosen abitrarily to satisfy equation* (48)*. In particular,*

$$\langle A_h(t)v_h, v_h\rangle_{L^2(\Omega;\mathbb{R}^n)} \leq -|v_h(\cdot)|^2_{\varepsilon_h} + \omega_h \|v_h(\cdot)\|^2_{L^2(\Omega;\mathbb{R}^n)}, \qquad \text{for } v_h \in V_h, \tag{59}$$

with the seminorm $|\cdot|_{\varepsilon_h}$ *defined on* $V_{h\star}$ *according to equation* (51c)*.*

Proof. The proof is almost identical to that of Lemma 3.4 in [38]. □

The last technical result concerns a bound on orthogonal subscales on the discrete operator $(A_h(t), V_{h\star})$, according to Proposition 3.1 below.

Proposition 3.1 (Boundedness on orthogonal subscales)**.** *The discrete operator* $(A_h(t), V_{h\star})$ *satisfies*

$$\left|\langle A_h(t)(v-\pi_h v), w_h\rangle_{L^2(\Omega;\mathbb{R}^n)}\right| \lesssim \|v(\cdot)-\pi_h v(\cdot)\|_{h\star}\,\|w_h(\cdot)\|_h\,, \qquad \text{for } (v,w_h)\in H^1(\Omega;\mathbb{R}^n)\times V_h, \tag{60}$$

where the norms $\|\cdot\|_h$ *and* $\|\cdot\|_{h\star}$ *are defined according to equations* (52a) *and* (52b)*, respectively.*

Proof. By observing that

$$\begin{aligned}
&\int_\Gamma (v(x)-\pi_h v(x))^{\mathrm{T}} C^{\mathrm{T}}(t)\,\mathrm{d}s \int_\Omega w_h(x)\,\mathrm{d}x \le \sqrt{\sup_{t\in[0,T]}\|C(t)\|^2}\,\|v(\cdot)-\pi_h v(\cdot)\|_{L^2(\Gamma;\mathbb{R}^n)}\,\|w_h(\cdot)\|_{L^2(\Omega;\mathbb{R}^n)}\\
&= \sqrt{\inf_{(x,t)\in\Gamma\times[0,T]}|a(x,t)\cdot\nu(x)|}\,\|v(\cdot)-\pi_h v(\cdot)\|_{L^2(\Gamma;\mathbb{R}^n)}\sqrt{\frac{\sup_{t\in[0,T]}\|C(t)\|^2}{\inf_{(x,t)\in\Gamma\times[0,T]}|a(x,t)\cdot\nu(x)|}}\,\|w_h(\cdot)\|_{L^2(\Omega;\mathbb{R}^n)}\\
&\lesssim |v(\cdot)-\pi_h v(\cdot)|_\eta\,\sqrt{\varepsilon_h}\,\|w_h(\cdot)\|_{L^2(\Omega;\mathbb{R}^n)} \lesssim \|v(\cdot)-\pi_h v(\cdot)\|_{h\star}\,\|w_h(\cdot)\|_h\,,
\end{aligned} \tag{61}$$

the result is a direct consequence of Lemma 2.30 in [38]. □

3.3. Stability and convergence of the space semi-discrete DGMs

Some elementary results may be derived concerning the stability and convergence of the space semi-discrete DGMs. For completeness, these are reported below without proof.

Theorem 3.1 (Stability of the space semi-discrete problem)**.** *Consider the space semi-discrete problem* (54) *and the discrete operator* $(A_h(t), V_{h\star})$ *defined according to equation* (53)*. It holds*

$$\|u_h(\cdot,t)\|_{L^2(\Omega;\mathbb{R}^n)} \le \mathrm{e}^{t/t_\star}\left(\|u_h(\cdot,0)\|_{L^2(\Omega;\mathbb{R}^n)} + \int_0^t \|f(\cdot,t')\|_{L^2(\Omega;\mathbb{R}^n)}\,\mathrm{d}t'\right), \qquad \text{for } t\in[0,T]. \tag{62}$$

Proof. By relying on standard arguments, the result may be deduced from an application of Grönwall-Bellman's inequality. □

Theorem 3.2 (Convergence of space semi-discrete DGMs)**.** *Consider the IBVP* (13) *and the space semi-discrete problem* (54) *and assume that the exact solution satisfies* $u\in C^0([0,T];H^{k+1}(\Omega;\mathbb{R}^n))$*. Then, the following estimate holds:*

$$\|u(\cdot,t)-u_h(\cdot,t)\|_{L^2(\Omega;\mathbb{R}^n)} + \left(\int_0^t |u(\cdot,t')-u_h(\cdot,t')|^2_{\frac{\varepsilon_h}{2}}\,\mathrm{d}t'\right)^{1/2} \lesssim \mathrm{e}^{C_{\mathrm{sta}}t/t_\star}\chi h^{k+1/2}, \qquad \text{for } t\in[0,T], \tag{63}$$

where

$$\chi \triangleq \sqrt{\eta_{\mathrm{c}}T}\,\|u(\cdot)\|_{C^0([0,T];H^{k+1}(\Omega;\mathbb{R}^n))}\,, \tag{64}$$

and the constant C_{sta} *is independent of* h *and the data* $f(x,t)$*,* $C(t)$*, and* $a(x,t)$*.*

Proof. Combining standard arguments with the polynomial approximation properties asserted by Lemmas 3.1 and 3.2, the result may be deduced from an application of Grönwall-Bellman's inequality. □

The error estimate in equation (63) is quasi-optimal, since the order of convergence of the L^2-norm of the error is $O(h^{k+1})$, whereas that of the boundary contributions is $O(h^{k+1/2})$ (on this matter, see, *e.g.*, [38]).

4. Time discretisation and explicit RK schemes

Typically, the semi-discrete problem formulated according to equation (54) needs to be discretised also in time in order to be solved numerically, leading to fully discrete DGMs. To this end, a fixed time step δt is considered in this paper such that $T = N\delta t$, with $N \in \mathbb{N}$. For $n \in \{0, \dots, N\}$, the discrete time is defined as $t^n = n\delta t$, and more generally the superscript is used to indicate functions evaluated at the discrete time $t = t^n$. For example, the solution to the IBVP evaluated at $t = t^n$ is denoted by $u(t^n) = u^n$, and similarly for the forcing term $f^n = f(t^n)$. In the same spirit, given a real number $\rho \in [0, 1]$, the solution evaluated at $t^n + \rho\delta t$ is indicated with $u^{n+\rho} = u(t^n + \rho\delta t)$, and so on for other time-dependent quantities.

The mild assumption

$$\delta t \leq t_\star, \tag{65}$$

with $t_\star$ as in equation (49), is also introduced the to facilitate the error analysis. In this context, a very common way of approximating the problem described by equation (54) consists in resorting to an explicit RK algorithm. A possible choice for formulating a general RK scheme of order s for the semi-discrete problem (54) is

$$k_i = A_h(t^n + c_i\delta t)\left(u_h^n + \delta t \sum_{j=1}^{s} a_{ij}k_j\right) + f_h(t^n + c_i\delta t), \qquad \text{for } i \in \{1, \dots, s\}, \tag{66a}$$

$$u_h^{n+1} = u_h^n + \sum_{i=1}^{s} b_i k_i. \tag{66b}$$

In equation (66), $(a_{ij})_{1\leq i,j\leq s}$ are real numbers, $(b_i)_{1\leq i\leq s}$ are real numbers satisfying $\sum_{i=1}^{s} b_i = 1$, and $(c_i)_{1\leq i\leq s}$ are real numbers in $[0, 1]$ such that $c_i = \sum_{j=1}^{s} a_{ij}$ for all $i \in \{1, \dots, s\}$. These quantities are conventionally collected in the so-called *Butcher's tableau*

$$\begin{array}{c|ccc} c_1 & a_{11} & \dots & a_{1s} \\ \vdots & \vdots & \ddots & \vdots \\ c_s & a_{s1} & \dots & a_{ss} \\ \hline & b_1 & \dots & b_s \end{array}. \tag{67}$$

In particular, RK schemes are explicit whenever $a_{ji} = 0$ for all $i \geq j$.

In the following, two examples of explicit RK schemes are discussed: the forward Euler algorithm (RK1), detailed in the next Section 4.1, and the two-stage RK2 algorithms, presented in Section 4.2. More specifically, concerning the RK1 method, the main result is only enounced, whereas the complete analysis is detailed for the RK2 schemes. Appendix B collects instead some numerical results concerning the convergence rate of Heun's third-order scheme, an example of an RK3 method.

4.1. Forward Euler scheme

The simplest, and perhaps most intuitive approximation to the semi-discrete problem (54) takes the form

$$\frac{u^{n+1} - u^n}{\delta t} = A_h^n u^n + f_h^n, \tag{68}$$

leading to the alternative representation

$$u^{n+1} = u^n + \delta t A_h^n u^n + \delta t f_h^n, \tag{69a}$$

$$u_h^0 = \pi_h u_0, \tag{69b}$$

which corresponds to an explicit RK1 scheme with Butcher's tableau

$$\begin{array}{c|c} 0 & 0 \\ \hline & 1 \end{array}. \tag{70}$$

The discrete equation (69) are already in a suitable form for the error analysis. The corresponding main convergence result is asserted by Theorem 4.1 below.

Theorem 4.1 (Convergence for the forward Euler scheme)**.** *Assume that* $u \in C^2([0,T];L^2(\Omega;\mathbb{R}^n)) \cap C^0([0,T];H^1(\Omega;\mathbb{R}^n))$ *and set* $V_h \triangleq \mathbb{P}_d^0(\mathcal{T}_h;\mathbb{R}^n)$*. Moreover, assume that the CFL condition*

$$\delta t \leq \varrho \frac{h}{\eta_c} \tag{71}$$

is satisfied with a suitable threshold $\varrho \in \mathbb{R}_{>0}$ *independent of* h*,* δt*, and the data* $f(x,t)$*,* $C(t)$ *and* $a(x,t)$*. Then, the following estimate holds:*

$$\left\|u^N(\cdot) - u_h^N(\cdot)\right\|_{L^2(\Omega;\mathbb{R}^n)} + \left(\sum_{n=0}^{N-1} \delta t \left|u^n(\cdot) - u_h^n(\cdot)\right|_{\frac{\varepsilon_h}{2}}^2\right)^{1/2} \lesssim \mathrm{e}^{C_\star T/t_\star}\left(\chi_1 \delta t + \chi_2 \sqrt{h}\right), \tag{72}$$

where

$$\chi_1 \triangleq \sqrt{t_\star T}\left\|\frac{\partial^2 u(\cdot,\cdot)}{\partial t^2}\right\|_{C^0([0,T];L^2(\Omega;\mathbb{R}^n))}, \tag{73a}$$

$$\chi_2 \triangleq \sqrt{\eta_c T}\left\|\frac{\partial^2 u(\cdot,\cdot)}{\partial t^2}\right\|_{C^0([0,T];H^1(\Omega;\mathbb{R}^n))}, \tag{73b}$$

the seminorm $|\cdot|_{\frac{\varepsilon_h}{2}}$ *is defined according to equation* (51d)*, and the constant* $C_\star$ *is independent of* h*,* δt*, and the data* $f(x,t)$*,* $C(t)$*, and* $a(x,t)$*.*

Proof. The proof builds upon similar steps of those required to prove Theorem 3.7 in [38], and is omitted for the sake of brevity. □

Remark 4.1. It is worth clarifying that the specific choice of the polynomial space $V_h \triangleq \mathbb{P}_d^0(\mathcal{T}_h;\mathbb{R}^n)$ in Theorem 4.1 is motivated by the fact that higher polynomial degrees require enforcing the 2-CFL condition (77) in order to provide optimal convergence. Since the forward Euler approximation is less than first-order accurate in space, such a requirement is too stringent, and is instead explored in the context of RK2 schemes. A more elaborated discussion concerning this aspect is reported in [38].

4.2. Explicit RK2 schemes

Concerning the semi-discrete problem (54), in the most general form, RK2 schems admit a general representation as in equation (66) according to

$$k_1 = A_h^n u_h^n + f_h^n, \tag{74a}$$

$$k_2 = A_h^{n+\lambda}(u_h^n + \lambda \delta t k_1) + f_h^{n+\lambda}, \tag{74b}$$

$$u_h^{n+1} = u_h^n + \left(1 - \frac{1}{2\lambda}\right)k_1 + \frac{1}{\lambda}k_2, \tag{74c}$$

with Butcher's tableau reading

$$\begin{array}{c|cc} 0 & 0 & 0 \\ \lambda & \lambda & 0 \\ \hline & 1-\frac{1}{2\lambda} & \frac{1}{\lambda} \end{array}, \tag{75}$$

where $\lambda \in [1/2, 1]$. In particular, the Butcher's tableau in equation (75) corresponds to the explicit midpoint method for $\lambda = 1/2$, to Heun's second-order method for $\lambda = 1$, and to Ralston's method for $\lambda = 2/3$.

Following the approach outlined by Shu and Osher [54], the representation of equation (74) may be converted into the following one by introducing intermediate steps on the solution:

$$w_h^n = u_h^n + \delta t A_h^n u_h^n + \delta t f_h^n, \tag{76a}$$

$$u_h^{n+1} = \frac{u_h^n}{2\lambda} + \left(1 - \frac{1}{2\lambda}\right) w_h^n + \frac{\delta t}{2} A_h^{n+\lambda} \left[\left(\frac{1}{\lambda} - 1\right) u_h^n + w_h^n\right] + \frac{\delta t}{2\lambda} f_h^{n+\lambda}, \tag{76b}$$

$$u_h^0 = \pi_h u_0, \tag{76c}$$

which is more convenient to proceed with the error analysis performed in Section 4.2. It is also worth observing that, whenever the operators $(A(t), D)$ and $(A_h(t), V_{h\star})$ are time-independent, yielding thus $A_h^n = A_h^{n+\lambda} = A_h$ in equations (76), all the above-mentioned methods admit a representation in the form (76) with $\lambda = 1$ (see, *e.g.*, [38]).

The corresponding main convergence result is asserted by Theorem 4.2 below.

Theorem 4.2 (Convergence for the explicit RK2 schemes)**.** *Assume that* $u \in C^3([0,T]; L^2(\Omega;\mathbb{R}^n)) \cap C^s([0,T]; H^{k+1-s}(\Omega;\mathbb{R}^n))$ *for* $s \in \{0,1\}$, $f \in C^2([0,T]; L^2(\Omega;\mathbb{R}^n))$, $A \in C^2([0,T]; \mathscr{L}(H^1(\Omega;\mathbb{R}^n); L^2(\Omega;\mathbb{R}^n)))$, *and set* $V_h \triangleq \mathbb{P}_d^k(\mathcal{T}_h;\mathbb{R}^n)$ *for* $k \geq 1$. *Moreover, assume that the 2-CFL condition*

$$\delta t \leq \varrho' \frac{1}{t_\star} \left(\frac{h}{\eta_c}\right)^2, \tag{77}$$

is satisfied with a suitable threshold $\varrho' \in \mathbb{R}_{>0}$ *independent of* h, δt, *and the data* $f(x,t)$, $C(t)$ *and* $a(x,t)$. *Then, the following estimate holds:*

$$\begin{aligned}\left\|u^N(\cdot) - u_h^N(\cdot)\right\|_{L^2(\Omega;\mathbb{R}^n)} + \left(\sum_{n=0}^{N-1} \frac{2\lambda - 1}{\lambda} \delta t \left|u^n(\cdot) - u_h^n(\cdot)\right|_{\frac{\varepsilon_h}{2}}^2 + \lambda \delta t \left|\frac{1-\lambda}{\lambda}(u^n(\cdot) - u_h^n(\cdot)) + w^n(\cdot) - w_h^n(\cdot)\right|_{\frac{\varepsilon_h}{2}}^2\right)^{1/2} \\ \lesssim \mathrm{e}^{C_\star T/t_\star}\left(\chi_1 \delta t^2 + \chi_2 \delta t^3 + \chi_3 h^{k+1/2}\right),\end{aligned} \tag{78}$$

where

$$\chi_1 \triangleq \sqrt{t_\star T} C_{fu}, \tag{79a}$$

$$\chi_2 \triangleq \sqrt{t_\star T} C_u, \tag{79b}$$

$$\chi_3 \triangleq \sqrt{\eta_c T} \sum_{s=0}^{1} \eta_c^{-s} \left\|\frac{\partial^s u(\cdot,\cdot)}{\partial t^s}\right\|_{C^0([0,T];H^{k+1-s}(\Omega;\mathbb{R}^n))}, \tag{79c}$$

the seminorm $|\cdot|_{\frac{\varepsilon_h}{2}}$ *is defined according to equation* (51d), *the constant* $C_\star$ *is independent of* h, δt, *and the data* $f(x,t)$, $C(t)$, *and* $a(x,t)$, *and* C_{fu} *and* C_u *are given by*

$$\begin{aligned}C_{fu} \triangleq \left\|\frac{\partial^3 u(\cdot,\cdot)}{\partial t^3}\right\|_{C^0([0,T];L^2(\Omega;\mathbb{R}^n))} + \eta_2 \left\|u(\cdot,\cdot)\right\|_{C^0([0,T];H^1(\Omega;\mathbb{R}^n))} \\ + \eta_1 \left\|\frac{\partial u(\cdot,\cdot)}{\partial t}\right\|_{C^0([0,T];H^1(\Omega;\mathbb{R}^n))} + \left\|\frac{\partial^2 f(\cdot,t)}{\partial t^2}\right\|_{C^0([0,T];L^2(\Omega;\mathbb{R}^n))},\end{aligned} \tag{80a}$$

$$C_u \triangleq \eta_2 \left\|\frac{\partial u(\cdot,\cdot)}{\partial t}\right\|_{C^0([0,T];H^1(\Omega;\mathbb{R}^n))}, \tag{80b}$$

with

$$\eta_1 \triangleq \max\left\{\sup_{t\in[0,T]} \left\|\frac{\partial a(\cdot,t)}{\partial t}\right\|_\infty, \sup_{t\in[0,T]} \left\|\frac{\mathrm{d}C(t)}{\mathrm{d}t}\right\|\right\}, \tag{81a}$$

$$\eta_2 \triangleq \max\left\{ \sup_{t\in[0,T]} \left\| \frac{\partial^2 a(\cdot,t)}{\partial t^2} \right\|_\infty , \sup_{t\in[0,T]} \left\| \frac{\mathrm{d}^2 C(t)}{\mathrm{d}t^2} \right\| \right\}. \tag{81b}$$

Proof. Building upon the results asserted in Lemmas 4.1–4.4, the proof is similar to that of Theorem 4.1, with the difference that the norm $\|\cdot\|_{h\star}$ should be replaced by $\|\cdot\|_{\star\star}$, and the term $\|\zeta_\pi^n(\cdot)\|_{\star\star}$ need to be accounted for, in addition to $\|\xi_\pi^n(\cdot)\|_{\star\star}$. The reader is redirected to [38] for further details. □

Remark 4.2. The main difference between Theorem 4.2 and the corresponding result established in [38] (Thm. 3.10) resides in the fact that the operators $(A(t), D)$ and $(A_h(t), V_{h\star})$ are time-varying. As a result, except for Heun's second-order method (corresponding to $\lambda = 1$), the discrete equation (76) cannot be recast in the same form as that studied in [38], and necessitate a dedicated analysis. An interesting conclusion is that, owing to the presence of time-varying operator $(A(t), D)$ and $(A_h(t), V_{h\star})$, optimal estimates may be achieved with the aid of the same techniques outlined in [38] owing to the more stringent 2-CFL condition (77), whereas only a 4/3-CFL condition, namely,

$$\delta t \leq \varrho t_\star^{-1/3} \left(\frac{h}{\eta_c} \right)^{4/3}, \tag{82}$$

for some $\varrho \in \mathbb{R}_{>0}$, is required in [38]. In this context, it is also worth observing that the 4/3-CFL condition (82) is implied by the 2-CFL one (77).

The next Section 4.3 delivers the proofs for Lemmas 4.1–4.4.

4.3. Error analysis for explicit RK2 schemes

The error analysis for the forward RK2 schemes follows a similar *iter* to that outlined in [38]. In particular, the first step consists in deducing of a discrete time equation governing the evolution of the approximation error.

4.3.1. Error equation

The present Section is devoted to deriving the error equation. In particular, by defining the quantities ξ_h^n and ξ_π^n as

$$\xi_h^n \triangleq u_h^n - \pi_h u^n, \tag{83a}$$
$$\xi_\pi^n \triangleq u^n - \pi_h u^n, \tag{83b}$$

and introducing

$$\zeta_h^n \triangleq w_h^n - \pi_h w^n, \tag{84a}$$
$$\zeta_\pi^n \triangleq w^n - \pi_h w^n, \tag{84b}$$

the errors may be decomposed as

$$u^n - u_h^n = \xi_\pi^n - \xi_h^n, \tag{85a}$$
$$w^n - w_h^n = \zeta_\pi^n - \zeta_h^n, \tag{85b}$$

with

$$w \triangleq u + \delta t \frac{\mathrm{d}u}{\mathrm{d}t}. \tag{86}$$

Starting with equations (83), (84), and (86), it is possible to derive the error equations as in the following Lemma 4.1, which implicitly presumes multiplying by functions $w_h \in V_h$ and taking the inner product on $L^2(\Omega;\mathbb{R}^n)$.

Lemma 4.1. *Assume that* $u \in C^3([0,T];L^2(\Omega;\mathbb{R}^n)) \cap C^1([0,T];H^1(\Omega;\mathbb{R}^n))$, $f \in C^2([0,T];L^2(\Omega;\mathbb{R}^n))$, *and* $A \in C^2([0,T];\mathscr{L}(H^1(\Omega;\mathbb{R}^n);L^2(\Omega;\mathbb{R}^n)))$. *Then, the error equation satisfies*

$$\zeta_h^n = \xi_h^n + \delta t A_h^n \xi_h^n - \delta t \alpha_h^n, \tag{87a}$$

$$\xi_h^{n+1} = \frac{\xi_h^n}{2\lambda} + \left(1 - \frac{1}{2\lambda}\right)\zeta_h^n + \frac{\delta t}{2} A_h^{n+\lambda}\left[\left(\frac{1}{\lambda} - 1\right)\xi_h^n + \zeta_h^n\right] - \frac{\delta t}{2}\beta_h^n, \tag{87b}$$

where

$$\alpha_h^n \triangleq A_h^n \xi_\pi^n, \tag{88a}$$

$$\beta_h^n \triangleq A_h^{n+\lambda}\left[\left(\frac{1}{\lambda} - 1\right)\xi_\pi^n + \zeta_\pi^n\right] - \delta t(\pi_h \Lambda^n u^n + \pi_h F^n) - \lambda \delta t^2 \pi_h \left(\frac{\mathrm{d}A^n}{\mathrm{d}t} + \Lambda^n\right)\frac{\mathrm{d}u^n}{\mathrm{d}t} + \pi_h \theta^n, \tag{88b}$$

with

$$\theta^n \triangleq \frac{1}{\delta t}\int_{t^n}^{t^{n+1}} \left(t^{n+1} - t\right)^2 \frac{\mathrm{d}^3 u(t)}{\mathrm{d}t^3}\,\mathrm{d}t, \tag{89a}$$

$$\Lambda^n \triangleq \frac{1}{\lambda \delta t}\int_{t^n}^{t^{n+\lambda}} \left(t^{n+\lambda} - t\right)\frac{\mathrm{d}^2 A(t)}{\mathrm{d}t^2}\,\mathrm{d}t, \tag{89b}$$

$$F^n \triangleq \frac{1}{\lambda \delta t}\int_{t^n}^{t^{n+\lambda}} \left(t^{n+\lambda} - t\right)\frac{\mathrm{d}^2 f(t)}{\mathrm{d}t^2}\,\mathrm{d}t. \tag{89c}$$

Proof. From Lemma 3.3, consistency at discrete time t^n yields

$$\pi_h w^n = \pi_h u^n + \delta t \pi_h \frac{\mathrm{d}u^n}{\mathrm{d}t} = \pi_h u^n + \delta t A_h^n u^n + \delta t f_h^n. \tag{90}$$

Subtracting the above equations (90) from (76a) and defining α_h^n according to (88a) provides (87a). Moreover, a second-order Taylor expansion with integral remainder gives

$$u^{n+1} = u^n + \delta t \frac{\mathrm{d}u^n}{\mathrm{d}t} + \frac{\delta t^2}{2}\frac{\mathrm{d}^2 u}{\mathrm{d}t^2} + \frac{\delta t}{2}\theta^n = w^n + \frac{\delta t}{2}A^n(w^n - u^n) + \frac{\delta t^2}{2}\frac{\mathrm{d}A^n}{\mathrm{d}t}u^n + \frac{\delta t^2}{2}\frac{\mathrm{d}f^n}{\mathrm{d}t} + \frac{\delta t}{2}\theta^n, \tag{91}$$

with θ^n reading as in equation (89a). Analogously, a first-order Taylor expansion with integral remainder of $A^{n+\lambda}$ gives

$$A^{n+\lambda} = A^n + \lambda \delta t \frac{\mathrm{d}A^n}{\mathrm{d}t} + \lambda \delta t \Lambda^n, \tag{92}$$

with Λ^n defined according to equation (89b). Substituting the latter expression into equation (91) and performing a similar first-order expansion for $f^{n+\lambda}$ provides, after some manipulations,

$$u^{n+1} = \frac{u^n}{2\lambda} + \left(1 - \frac{1}{2\lambda}\right)w^n + \frac{\delta t}{2}A^{n+\lambda}\left[\left(\frac{1}{\lambda} - 1\right)u^n + w^n\right] + \frac{\delta t}{2}\delta^n, \tag{93}$$

with

$$\begin{aligned}\delta^n &\triangleq -\delta t(\Lambda^n u^n + F^n) + \left(A^{n+\lambda} - A^n\right)(u^n - w^n) + \frac{f^{n+\lambda}}{\lambda} + \theta^n \\ &= -\delta t(\Lambda^n u^n + F^n) - \lambda \delta t^2 \left(\frac{\mathrm{d}A^n}{\mathrm{d}t} + \Lambda^n\right)\frac{\mathrm{d}u^n}{\mathrm{d}t} + \frac{f^{n+\lambda}}{\lambda} + \theta^n,\end{aligned} \tag{94}$$

where F^n reads as in equation (89c).

Projecting equation (93) onto V_h and invoking the time-shifted consistency property proved in Lemma 3.3 for both $A_h^{n+\lambda}u$ and $A_h^{n+\lambda}w$ therefore yields

$$\pi_h u^{n+1} = \frac{\pi_h u^n}{2\lambda} + \left(1 - \frac{1}{2\lambda}\right)\pi_h w^n + \frac{\delta t}{2} A_h^{n+\lambda}\left[\left(\frac{1}{\lambda} - 1\right)u^n + w^n\right] + \frac{\delta t}{2}\pi_h \delta^n, \tag{95}$$

in which

$$\pi_h \delta^n \triangleq -\delta t(\pi_h \Lambda^n u^n + \pi_h F^n) - \lambda \delta t^2 \pi_h \left(\frac{\mathrm{d}A^n}{\mathrm{d}t} + \Lambda^n\right)\frac{\mathrm{d}u^n}{\mathrm{d}t} + \frac{f_h^{n+\lambda}}{\lambda} + \pi_h \theta^n. \tag{96}$$

Subtracting equation (95) from (76b) and defining β_h^n as in (88b) gives the desired result. □

4.3.2. Energy estimate

The next step involves obtaining an energy estimate for the term ξ_h^{n+1} appearing in equation (87b). The result is formalised in Lemma 4.2 below.

Lemma 4.2 (Energy estimate)**.** *The error equation* (87) *satisfy the following energy estimate:*

$$\begin{aligned}
&\left\|\xi_h^{n+1}(\cdot)\right\|_{L^2(\Omega;\mathbb{R}^n)}^2 + \frac{2\lambda-1}{\lambda}\delta t\left|\xi_h^n(\cdot)\right|_{\varepsilon_h}^2 + \lambda\delta t\left|\frac{1-\lambda}{\lambda}\xi_h^n(\cdot) + \zeta_h^n(\cdot)\right|_{\varepsilon_h}^2 \\
&\qquad \le (1-\lambda)\left\|\xi_h^{n+1}(\cdot) - \xi_h^n(\cdot)\right\|_{L^2(\Omega;\mathbb{R}^n)}^2 + \lambda\left\|\xi_h^{n+1}(\cdot) - \zeta_h^n(\cdot)\right\|_{L^2(\Omega;\mathbb{R}^n)}^2 \\
&\qquad\quad + \left(1 + \frac{2\lambda-1}{\lambda}\delta t\omega_h\right)\left\|\xi_h^n(\cdot)\right\|_{L^2(\Omega;\mathbb{R}^n)}^2 + \lambda\delta t\omega_h\left\|\frac{1-\lambda}{\lambda}\xi_h^n(\cdot) + \zeta_h^n(\cdot)\right\|_{L^2(\Omega;\mathbb{R}^n)}^2 \\
&\qquad\quad - \frac{2\lambda-1}{\lambda}\delta t\langle\alpha_h^n, \xi_h^n\rangle_{L^2(\Omega;\mathbb{R}^n)} - \lambda\delta t\left\langle\beta_h^n, \frac{1-\lambda}{\lambda}\xi_h^n + \zeta_h^n\right\rangle_{L^2(\Omega;\mathbb{R}^n)},
\end{aligned} \tag{97}$$

where the constant ω_h is given as in equation (58).

Proof. See Appendix A.1. □

4.3.3. Preliminary stability bounds

The next result, formalised in Lemma 4.3, delivers some preliminary stability bounds that are necessary to ensure stability and convergence of the considered RK2 schemes.

For what follows, the additional norm is introduced on $V_{h\star}$:

$$\|v(\cdot)\|_{\star\star}^2 \triangleq \|v(\cdot)\|_{h\star}^2 + \eta_c h\sum_{i=1}^n \|\nabla_h v_i(\cdot)\|_{L^2(\Omega;\mathbb{R}^n)}^2. \tag{98}$$

Furthermore, to allow for ease of notation, the following energy-like quantity, collecting the contributions of the space and time approximation errors, is defined:

$$\mathscr{E}_h^n \triangleq \|\xi_\pi^n(\cdot)\|_{\star\star} + \|\zeta_\pi^n(\cdot)\|_{\star\star} + \sqrt{t_\star}\left(C_{fu}\delta t^2 + C_u\delta t^3\right) + \frac{1}{\sqrt{t_\star}}\|\xi_h^n(\cdot)\|_{L^2(\Omega;\mathbb{R}^n)}. \tag{99}$$

where C_{fu} and C_u read as in equation (80).

Lemma 4.3 (Preliminary stability bounds)**.** *Assume that $u \in C^3([0,T];L^2(\Omega;\mathbb{R}^n)) \cap C^1([0,T];H^1(\Omega;\mathbb{R}^n))$, $f \in C^2([0,T];L^2(\Omega;\mathbb{R}^n))$, and $A \in C^2([0,T];\mathscr{L}(H^1(\Omega;\mathbb{R}^n);L^2(\Omega;\mathbb{R}^n)))$. Then, if the CFL condition in equation* (71) *holds, there exists $C_\star$ independent of h, δt, and the data $f(x,t)$, $C(t)$, and $a(x,t)$ such that*

$$\begin{aligned}
&\left\|\xi_h^{n+1}(\cdot)\right\|_{L^2(\Omega;\mathbb{R}^n)}^2 + \frac{2\lambda-1}{2\lambda}\delta t\left|\xi_h^n(\cdot)\right|_{\frac{\varepsilon_h}{2}}^2 + \frac{\lambda}{2}\delta t\left|\frac{1-\lambda}{\lambda}\xi_h^n(\cdot) + \zeta_h^n(\cdot)\right|_{\frac{\varepsilon_h}{2}}^2 \\
&\qquad \lesssim \|\xi_h^n(\cdot)\|_{L^2(\Omega;\mathbb{R}^n)}^2 + (1-\lambda)\left\|\xi_h^{n+1}(\cdot) - \xi_h^n(\cdot)\right\|_{L^2(\Omega;\mathbb{R}^n)} + \lambda\left\|\xi_h^{n+1}(\cdot) - \zeta_h^n(\cdot)\right\|_{L^2(\Omega;\mathbb{R}^n)} + C_\star\delta t(\mathscr{E}_h^n)^2.
\end{aligned} \tag{100}$$

Proof. See Appendix A.2. □

4.3.4. Stability

Stability for the RK2 schemes is finally proved by inferring opportune bounds on the anti-dissipative terms appearing on the right-hand side of energy estimate in equation (97). To this end, the 2-CFL condition (77) is invoked. Lemma 4.4 asserts the result.

Lemma 4.4 (Stability of RK2 schemes)**.** *Assume that* $u \in C^3([0,T];L^2(\Omega;\mathbb{R}^n)) \cap C^1([0,T];H^1(\Omega;\mathbb{R}^n))$*,* $f \in C^2([0,T];L^2(\Omega;\mathbb{R}^n))$*, and* $A \in C^2([0,T];\mathscr{L}(H^1(\Omega;\mathbb{R}^n);L^2(\Omega;\mathbb{R}^n)))$*. Then, if the 2-CFL condition in equation (77) holds for some* $\varrho' \in \mathbb{R}_{>0}$*, there exists* $C_\star$ *independent of* h*,* δt*, and the data* $f(x,t)$*,* $C(t)$*, and* $a(x,t)$ *such that*

$$\left\|\xi_h^{n+1}(\cdot)\right\|^2_{L^2(\Omega;\mathbb{R}^n)} + \frac{2\lambda-1}{2\lambda}\delta t\,|\xi_h^n(\cdot)|^2_{\frac{\varepsilon_h}{2}} + \frac{\lambda}{2}\delta t\left|\frac{1-\lambda}{\lambda}\xi_h^n(\cdot)+\zeta_h^n(\cdot)\right|^2_{\frac{\varepsilon_h}{2}} \leq \|\xi_h^n(\cdot)\|^2_{L^2(\Omega;\mathbb{R}^n)} + C_\star\delta t(\mathscr{E}_h^n)^2, \tag{101}$$

where the seminorm $|\cdot|_{\frac{\varepsilon_h}{2}}$ *reads as in equation (51d).*

Proof. From the error equation (87b), it is possible to deduce that

$$\xi_h^{n+1}-\zeta_h^n = \frac{\delta t}{2}A_h^{n+\lambda}\left(\frac{1-\lambda}{\lambda}\xi_h^n+\zeta_h^n\right) - \frac{\delta t}{2\lambda}A_h^n\xi_h^n + \frac{\delta t}{2\lambda}\alpha_h^n - \frac{\delta t}{2}\beta_h^n. \tag{102}$$

Substituting the expression for $\zeta_h^n(x)$ from equation (87a) also yields

$$\xi_h^{n+1}-\zeta_h^n = \frac{\delta t^2}{2}A_h^{n+\lambda}A_h^n\xi_h^n + \frac{\delta t}{2\lambda}\left(A_h^{n+\lambda}-A_h^n\right)\xi_h^n + \frac{\delta t}{2\lambda}\left(\alpha_h^n - \lambda\delta t A_h^{n+\lambda}\alpha_h^n - \lambda\beta_h^n\right). \tag{103}$$

Recalling that $\delta t \leq t_\star$, the last quantity appearing on the right-hand side may be bounded with the aid of the estimates in equations (A.11), (A.12), and (A.17) as

$$\begin{aligned}|\mathscr{T}_3| &\triangleq \frac{\delta t}{2\lambda}\left\|\alpha_h^n(\cdot)-\lambda\delta t A_h^{n+\lambda}\alpha_h^n(\cdot)-\lambda\beta_h^n(\cdot)\right\|_{L^2(\Omega;\mathbb{R}^n)}\\ &\leq \frac{\delta t}{2\lambda}\|\alpha_h^n(\cdot)\|_{L^2(\Omega;\mathbb{R}^n)} + \frac{\delta t^2}{2}\left\|A_h^{n+\lambda}\alpha_h^n(\cdot)\right\|_{L^2(\Omega;\mathbb{R}^n)} + \frac{\delta t}{2}\|\beta_h^n(\cdot)\|_{L^2(\Omega;\mathbb{R}^n)}\\ &\lesssim \delta t\,\|\alpha_h^n(\cdot)\|_{L^2(\Omega;\mathbb{R}^n)} + \delta t\,\|\beta_h^n(\cdot)\|_{L^2(\Omega;\mathbb{R}^n)} \lesssim \sqrt{\delta t}\mathscr{E}_h^n.\end{aligned} \tag{104}$$

Concerning the second term, combining the bound in equation (A.11) with the 2-CFL condition (77), it may be immediately deduced that

$$\begin{aligned}|\mathscr{T}_2| &\triangleq \frac{\delta t}{2\lambda}\left\|\left(A_h^{n+\lambda}-A_h^n\right)\xi_h^n(\cdot)\right\|_{L^2(\Omega;\mathbb{R}^n)} \leq \frac{\delta t}{2\lambda}\left\|A_h^{n+\lambda}\xi_h^n(\cdot)\right\|_{L^2(\Omega;\mathbb{R}^n)} + \frac{\delta t}{2\lambda}\|A_h^n\xi_h^n(\cdot)\|_{L^2(\Omega;\mathbb{R}^n)}\\ &\lesssim \delta t\frac{\eta_c}{h}\|\xi_h^n(\cdot)\|_{L^2(\Omega;\mathbb{R}^n)} \lesssim \sqrt{\delta t}\mathscr{E}_h^n.\end{aligned} \tag{105}$$

Finally, the first quantity may be bounded by applying two times the estimate (77) and invoking the 4/3-CFL condition (82) (which is implied by the 2-CFL condition in Eq. (77)). This yields

$$|\mathscr{T}_1| \triangleq \frac{\delta t^2}{2}\left\|A_h^{n+\lambda}A_h^n\xi_h^n(\cdot)\right\|_{L^2(\Omega;\mathbb{R}^n)} \lesssim \delta t^2\left(\frac{\eta_c}{h}\right)^2\|\xi_h^n(\cdot)\|_{L^2(\Omega;\mathbb{R}^n)} \lesssim \sqrt{\delta t}\mathscr{E}_h^n. \tag{106}$$

Therefore, combining equations (104), (105), and (106) provides

$$\left\|\xi_h^{n+1}(\cdot)-\zeta_h^n(\cdot)\right\|^2_{L^2(\Omega;\mathbb{R}^n)} \lesssim |\mathscr{T}_1|^2 + |\mathscr{T}_2|^2 + |\mathscr{T}_3|^2 \lesssim \delta t(\mathscr{E}_h^n)^2. \tag{107}$$

Similarly, also from the error equation (87b), it may be inferred that

$$\xi_h^{n+1} - \xi_h^n = \left(1 - \frac{1}{2\lambda}\right)\delta t A_h^n \xi_h^n + \frac{\delta t}{2\lambda}(A_h^{n+\lambda} - A_h^n)\xi_h^n - \frac{\delta t}{2}\left[\left(1 - \frac{1}{2\lambda}\right)\alpha_h^n + \delta t A_h^{n+\lambda}\alpha_h^n + \beta_h^n\right]. \tag{108}$$

Therefore, following a similar rationale as in the derivation of equation (107), it may be concluded that

$$\left\|\xi_h^{n+1}(\cdot) - \xi_h^n(\cdot)\right\|^2_{L^2(\Omega;\mathbb{R}^n)} \lesssim \delta t(\mathscr{E}_h^n)^2. \tag{109}$$

Adding equations (107) and (109) together yields the result. □

Remark 4.3. It is worth observing that, in the proof of Lemma 4.4 above, concerning the derivation of equation (107), the 2-CFL condition (77) was invoked only to provide an upper bound on the term $\mathscr{T}_2$. If the operators $(A(t), D)$ and $(A_h(t), V_{h\star})$ do not depend upon the time variable, the quantity $\mathscr{T}_2$ vanishes. Moreover, all the RK2 schemes analysed in the paper reduce to the form considered in [38], which may be obtained directly from equation (76) be specifying $\lambda = 1$. Accordingly, the contribution relating to $\left\|\xi_h^{n+1}(\cdot) - \xi_h^n(\cdot)\right\|^2_{L^2(\Omega;\mathbb{R}^n)}$ disappears from the energy estimate deduced as in equation (97). In this case, the less stringent 4/3-CFL condition (82) might be invoked.

5. Numerical experiments

For the sake of simplicity, the numerical experiments presented in the following are limited to problems in one space dimension that include boundary and trace terms, as those analysed in Section 2.2. Results about IBVPs in several space dimensions may instead be found in [39].

5.1. Analysis for smooth solutions

The hyperbolic problems typically encountered in rolling contact mechanics do not enjoy sufficient regularity to satisfy the conditions required by Theorem 4.2. Therefore, to verify numerically the theoretical bound derived according to Theorem 4.2, simplified IBVPs are first considered. The effect of boundary terms and time-varying operators are investigated separately in Sections 5.1.1 and 5.1.2, respectively.

5.1.1. Effect of boundary terms

In order to investigate numerically the rate of convergence for the total error predicted by Theorem 4.2, it may first be beneficial to consider equation (8) in the scalar case, *i.e.*, $u(x,t) \in \mathbb{R}$, with constant data $a(x,t) = a = 1$, $B(t) = B = 0$, $C(t) = C = 1/2$, and $f(x,t) = f = 0$. With this choice for the transport velocity $a(x,t)$, the matrix $C(t)$, and the forcing term $f(x,t)$, Assumption 2.1 holds for all $t \in [0,T]$ and consequently the problem admits a unique strict solution, as asserted by Theorem 2.1. In fact, since the transport velocity is constant, the corresponding IBVP problem admits a closed-form solution, consisting of an integral expression combined with a delay-differential equation (DDE) for the boundary term $u(1,t)$ [32]. In particular, sufficiently smooth solutions as those required by Theorem 4.2 may be derived owing to opportune assumptions made on the regularity of the IC, which may be prescribed as

$$u_0(x) = x^3 + \frac{3}{2}x^2 + \frac{5}{2}x, \qquad \text{for } x \in [0,1], \tag{110}$$

to satisfy the compatibility condition up to the second order both in time and space.

The total error, calculated using the expression appearing on the left-hand side of equation (78) by specifying $\psi_h = 3/2$, is reported in Table 1 for decreasing values of the meshsize h and polynomial degrees $k = 1$ and 2, considering explicit RK2 schemes with $\lambda = 1$ (corresponding to Heun's second-order method) owing to the refined 4/3-CFL condition (82) with $\varrho = 0.2$. In fact, it is worth emphasising that, when the problem data are constant, the operators $(A(t), D)$ and $(A_h(t), V_{h\star})$ are also time-independent, and, according to Remark 4.3, the

TABLE 1. Error convergence for polynomial degrees $k = 1$ and 2 predicted using Heun's second-order method ($\lambda = 1$) for the IBVP described by equations (8) and (110).

Meshsize h	Total error ($k = 1$)	Total error ($k = 2$)
0.025	0.0015	$5.59 \cdot 10^{-6}$
0.017	$8.59 \cdot 10^{-4}$	$2.00 \cdot 10^{-6}$
0.0125	$5.63 \cdot 10^{-4}$	$9.73 \cdot 10^{-7}$
0.01	$3.92 \cdot 10^{-4}$	$5.56 \cdot 10^{-7}$

4/3-CFL condition (82) may be more conveniently invoked in place of the 2-CFL one to derive quasi-optimal error convergence for the complete discrete RK2 schemes. Therefore, according to Theorem 4.2, under the refined 4/3-CFL condition (82), the RK2 scheme with polynomial degree $k = 1$ produces an error convegence in the order of $O(h^{8/3} + h^{3/2})$, whereas the polynomial degree $k = 2$ yields $O(h^{8/3} + h^{5/2})$ accuracy. In both case, the time error, relating to the contribution $h^{8/3}$, is dominated by that produced by the space discretisation, proportional to either $h^{3/2}$ or $h^{5/2}$. The values reported in Table 1 and the trends illustrated in Figure 1 seem to confirm the bound derived according to Theorem 4.2 to be sharp.

The maximum simulation times, corresponding to a meshsize of $h = 0.01$ with 100 elements simulated in MATLAB/Simulink® on a personal computer, amounted to 1.94 and 4.48 s for $k = 1$ and $k = 2$, respectively.

5.1.2. Effect of time-varying operators

To investigate numerically the effect connected with the presence of a time-varying operator, equation (8) are again considered in the scalar case, *i.e.*, $u(x,t) \in \mathbb{R}$, with $B(t) = B = 0$, $C(t) = C = 0$, $f(x,t) = f = 0$, and transport velocity and IC assigned as

$$a(x,t) = a(t) = 1 + t, \qquad \text{for } t \in [0,T], \tag{111a}$$
$$u_0(x) = x^3, \qquad \text{for } x \in [0,1]. \tag{111b}$$

The above expressions for the transport velocity and IC ensure the existence and uniqueness of sufficiently smooth solutions satisfying the assumptions of Theorem 4.2.

The total error, calculated as in the right-hand side of equation (78), is reported in Table 2 for decreasing values of the meshsize h and polynomial degrees $k = 1$ and 2, using Heun's method for time discretisation (RK2 schemes with $\lambda = 1$), with timestep δt obeying the 2-CFL condition of equation (77) with $\varrho' = 5$ and 10 for $k = 1$ and 2, respectively. Figure 2 seems to numerically corroborate that the bound derived in Theorem 4.2 is sharp. In particular, it is evident that, especially concerning the RK scheme with polynomial degree $k = 2$, the refined 4/3-CFL condition (82) is not sufficient to ensure the optimal rate of convergence predicted by Theorem 4.2.

The maximum simulation times, corresponding to a meshsize of $h = 0.0125$ with 80 elements, amounted to 1.57 and 3.15 s for $k = 1$ and $k = 2$, respectively.

5.2. Application to linear hyperbolic rolling contact problems

As an application from rolling contact mechanics, the problem described in Example 2.1 is considered. Restricting the attention to the scalar case, *i.e.*, $u(x,t) \in \mathbb{R}$, typical expressions for the time-dependent transport velocity $a(x,t)$, matrix $C(t)$ and forcing term $f(x,t)$ read according to equation (10), with $\varphi(t) = 0$ and

$$\alpha(t) = \alpha_0 + \alpha_\mathrm{I} \sin(\omega t), \tag{112a}$$
$$\sigma(t) = \sigma_0 + \sigma_\mathrm{I} \sin(\omega t), \tag{112b}$$

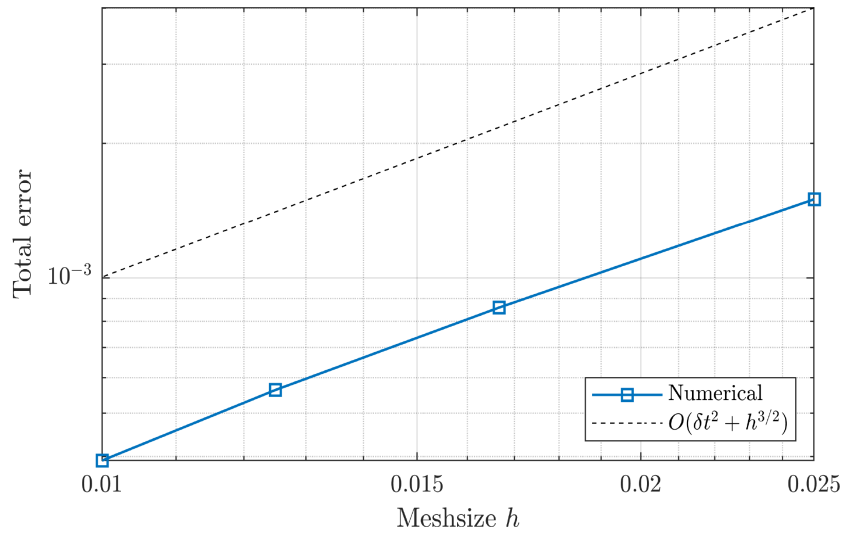

(a)

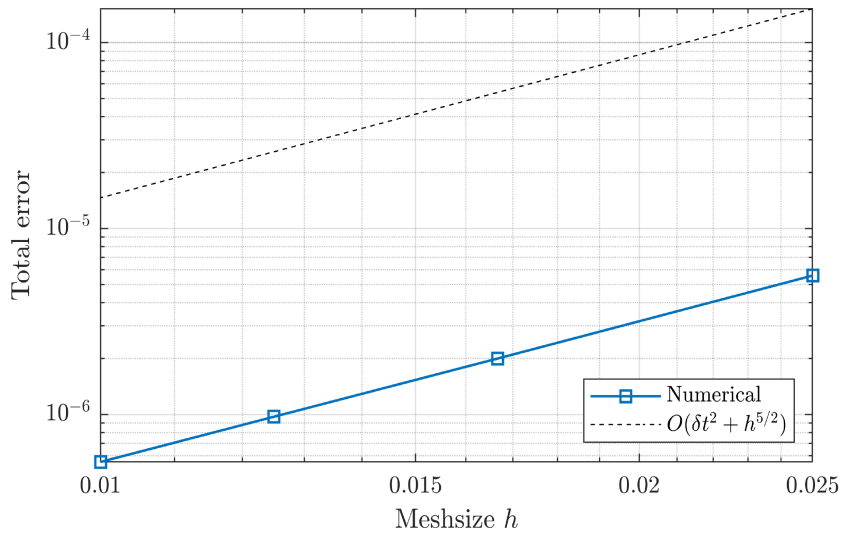

(b)

FIGURE 1. Convergence of the total error for different polynomial degrees $k = 1$ and 2 for the IBVP described by equations (8) and (110). (a) Convergence of the total error predicted according to Theorem 4.2 (polynomial degree $k = 1$). (b) Convergence of the total error predicted according to Theorem 4.2 (polynomial degree $k = 2$).

TABLE 2. Error convergence for polynomial degrees $k = 1$ and 2 predicted using Heun's second-order method ($\lambda = 1$) for the IBVP described by equations (8) and (111).

Meshsize h	Total error ($k = 1$, 4/3-CFL)	Total error ($k = 1$, 2-CFL)
0.05	$1.12 \cdot 10^{-2}$	$8.41 \cdot 10^{-3}$
0.025	$4.04 \cdot 10^{-3}$	$2.81 \cdot 10^{-3}$
0.0125	$1.60 \cdot 10^{-3}$	$8.54 \cdot 10^{-4}$
Meshsize h	Total error ($k = 2$, 4/3-CFL)	Total error ($k = 2$, 2-CFL)
0.05	$1.10 \cdot 10^{-2}$	$7.82 \cdot 10^{-3}$
0.025	$4.03 \cdot 10^{-3}$	$1.61 \cdot 10^{-3}$
0.0125	$1.60 \cdot 10^{-3}$	$2.99 \cdot 10^{-4}$

where both signals are characterised by the same frequency ω. Similar expressions for the transport velocity and rigid slip as those in equation (112) are typically connected with oscillating normal and tangential forces [55–57].

Figure 3 illustrates the numerical solution obtained using first and second-order polynomial functions ($k = 1$ and 2, respectively) in conjunction with Heun's second-order method in time. In both cases, the plotted solutions refer to a mesh with 10 elements, with $\varrho' = 0.2$ in equation (77). It may be observed that the trend predicted by the DGM with $k = 2$ is much smoother than that yielded by the lower-order polynomial degree. The total simulation time amounted to 14.92 and 25.46 s for $k = 1$ and 2. In this case, the heavier computational cost should be ascribed to the more stringent 2-CFL condition in equation (77) than the 4/3-one invoked previously concerning the problem with constant transport velocity.

For the IBVP described by equations (8) and (10), the error convergence is illustrated in Figure 4 for the usual polynomial degrees $k = 1$ and 2, respectively. As observed previously, the low regularity of the exact solution does not fulfil the criteria required by Theorem 4.2, and hence the rate of convergence is not optimal. In fact, the accuracy is approximately in the order of $O(h^{1/2})$. Concerning the problem under investigation, the simulation time was also prohibitive, amounting at more than 420 s for the smallest meshsize $h = 0.033$ in combination with the 2-CFL condition of equation (77).

6. Conclusions

The present paper addressed the problem of recovering numerical solutions to linear hyperbolic IBVPs encountered in rolling contact mechanics. Given the peculiar structure of the hyperbolic PDEs under investigation, which included integral and boundary terms in the one-dimensional case, the first part of the work was dedicated to establishing the well-posedness of the corresponding IBVPs. Existence and uniqueness were proved for the continuous problem within the mathematical framework provided by the semigroup theory. This allowed, in most cases, to derive strict solutions enjoying sufficient regularity properties to satisfy the assumptions required for the subsequent numerical analyses. With respect to problems involving several space dimensions, a classic result by Bardos [49] was conveniently recalled which applies to the governing equations of spinning and rolling bodies.

The second part of the paper was then devoted to the development of numerical schemes to approximate the exact solutions of the rolling contact problems described in Section 2. In particular, this was accomplished by combining discontinuous Galerkin finite element methods (DGMs) with explicit Runge–Kutta (RK) algorithms of first and second-order. Whilst the semi-discrete problem and the discrete operator were introduced and analysed in Section 3, the complete discrete formulation was fully developed in Section 4, where the two main results were also asserted regarding the convergence of the proposed schemes. More specifically, departing from the analyses initiated in [38,39], analogous convergence results were established in the case of time-independent continuous and discrete operators $(A(t), D)$ and $(A_h(t), V_{h\star})$ when accounting for the presence of integral and

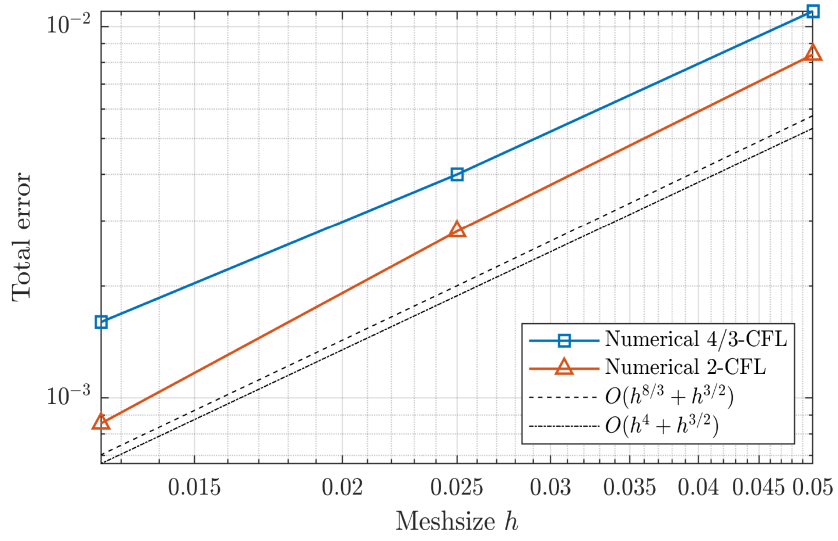

(a)

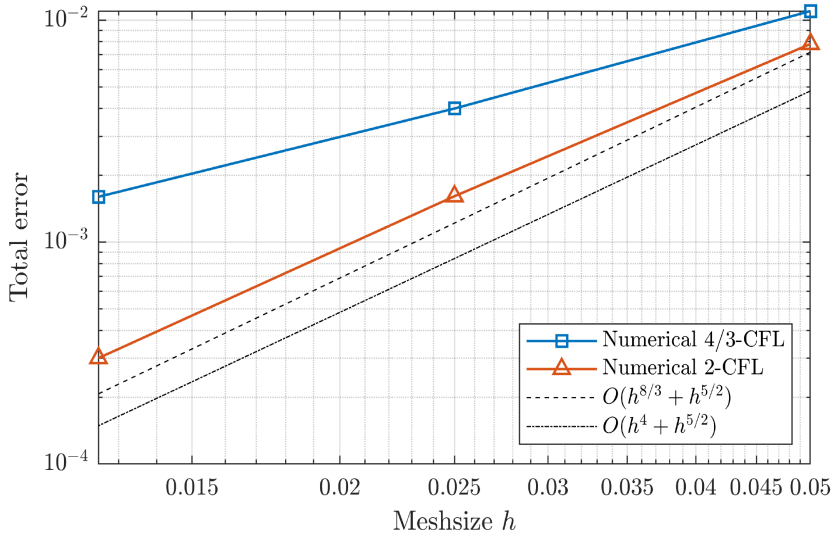

(b)

FIGURE 2. Convergence of the total error for different polynomial degrees $k = 1$ and 2 for the IBVP described by equations (8) and (111). (a) Convergence of the total error predicted according to Theorem 4.2 (polynomial degree $k = 1$). (b) Convergence of the total error predicted according to Theorem 4.2 (polynomial degree $k = 2$).

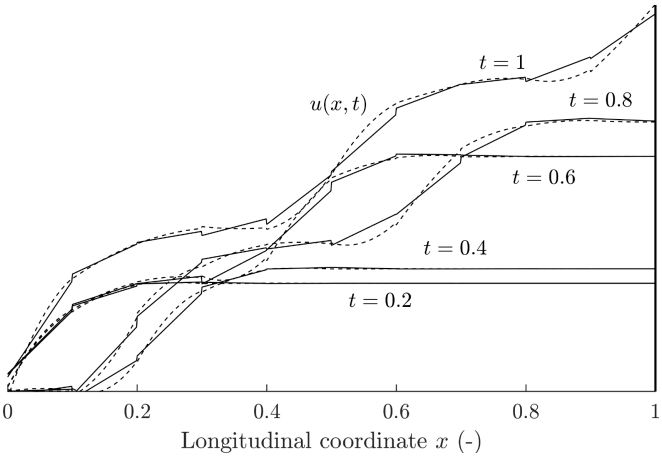

FIGURE 3. DGM approximations to the rolling contact problem described by equations (8) and (10), with time varying-data according to equation (112). Solid line: RK2 with polynomial degree $k = 1$ and 10 mesh elements; dashed line: RK2 with polynomial degree $k = 2$ and 10 mesh elements. Model parameters: $\alpha_0 = 0.075$, $\alpha_{\mathrm{I}} = 0.1 \cdot \alpha_0$, $M = 4.44$, $\sigma_0 = 0.7$, $\sigma_{\mathrm{I}} = 0.1 \cdot \sigma_0$, $\varphi = 0$, $\omega = 100$. Total simulation time $T = 2(\alpha_0 + \alpha_{\mathrm{I}})$.

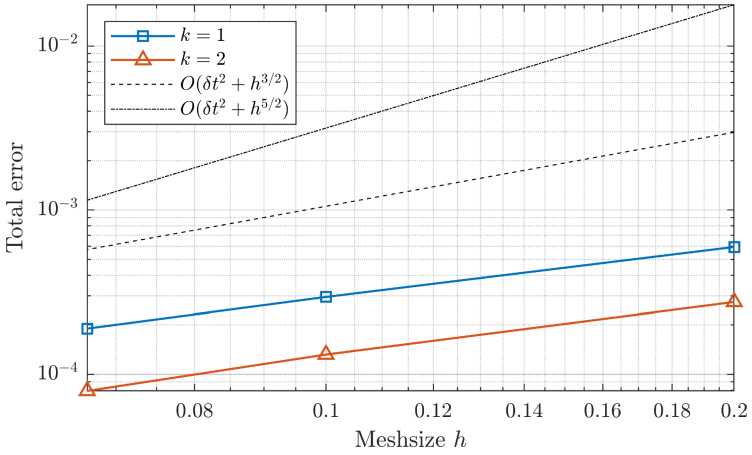

FIGURE 4. Convergence of the total error for different polynomial degrees $k = 1$ and 2 for the rolling contact problem described by equations (8) and (10), with time varying-data according to equation (112).

boundary terms. In particular, under the assumption of sufficiently smooth exact solutions and owing to a refined 4/3-CFL condition, accuracy in the order of $O(h^{4/3}+h^{1/2})$ and $O(h^{8/3}+h^{k+1/2})$ was asserted respectively for the finite-volume approximation in combination with RK1 algorithms, and for the DGMs in conjunction with RK2 schemes. The more involved case of time-dependent operators $(A(t), D)$ and $(A_h(t), V_{h\star})$ yielded similar results in terms of convergence rate, but required instead a stricter 2-CFL condition to hold. Numerical experiments, corroborating the theoretical analyses conducted in Section 4, were reported in Section 5 regarding some one-dimensional problems accounting for the presence of boundary and integral terms.

Future research efforts may be directed to the analysis of higher-order RK schemes, which are already available in virtual environments like MATLAB/Simulink®, and possibly able to overcome the drawbacks connected with too stringent CFL conditions, as also preliminarily suggested by the numerical experiments reported in Appendix B.

Appendix A. Technical proofs

Some technical proofs concerning the numerical schemes are collected here.

A.1. Proof of Lemma 4.2

The proof of Lemma 4.2 is given below.

Proof of Lemma 4.2. Taking the inner product of equation (87a) with $(2\lambda-1)/\lambda\xi_h^n(x)$ on $L^2(\Omega;\mathbb{R}^n)$ provides

$$\langle \xi_h^n, \zeta_h^n\rangle_{L^2(\Omega;\mathbb{R}^n)} = \|\xi_h^n(\cdot)\|^2_{L^2(\Omega;\mathbb{R}^n)} + \delta t\langle A_h^n\xi_h^n, \xi_h^n\rangle_{L^2(\Omega;\mathbb{R}^n)} - \delta t\langle \alpha_h^n, \xi_h^n\rangle_{L^2(\Omega;\mathbb{R}^n)}. \tag{A.1}$$

Similarly, taking the inner product of equation (87b) with $2(1-\lambda)\xi_h^k(x)+2\lambda\zeta_h^k(x)$ on $L^2(\Omega;\mathbb{R}^n)$ yields

$$\begin{aligned} 2(1-\lambda)\big\langle \xi_h^{n+1}, \xi_h^n\big\rangle_{L^2(\Omega;\mathbb{R}^n)} + 2\lambda\big\langle \xi_h^{n+1}, \zeta_h^n\big\rangle_{L^2(\Omega;\mathbb{R}^n)} &= \frac{1-\lambda}{\lambda}\|\xi_h^n(\cdot)\|^2_{L^2(\Omega;\mathbb{R}^n)} + (2\lambda-1)\|\zeta_h^n(\cdot)\|^2_{L^2(\Omega;\mathbb{R}^n)} \\ &+ \frac{4\lambda-2\lambda^2-1}{\lambda}\langle \xi_h^n, \zeta_h^n\rangle_{L^2(\Omega;\mathbb{R}^n)} + \lambda\delta t\left\langle A_h^{n+\lambda}\left(\frac{1-\lambda}{\lambda}\xi_h^n+\zeta_h^n\right), \frac{1-\lambda}{\lambda}\xi_h^n+\zeta_h^n\right\rangle_{L^2(\Omega;\mathbb{R}^n)} \\ &- \lambda\delta t\left\langle \beta_h^n, \frac{1-\lambda}{\lambda}\xi_h^n+\zeta_h^n\right\rangle_{L^2(\Omega;\mathbb{R}^n)}. \end{aligned} \tag{A.2}$$

Observing that

$$2\big\langle \xi_h^{n+1}, \xi_h^n\big\rangle_{L^2(\Omega;\mathbb{R}^n)} = \big\|\xi_h^{n+1}(\cdot)\big\|^2_{L^2(\Omega;\mathbb{R}^n)} + \|\xi_h^n(\cdot)\|^2_{L^2(\Omega;\mathbb{R}^n)} - \big\|\xi_h^{n+1}(\cdot)-\xi_h^n(\cdot)\big\|^2_{L^2(\Omega;\mathbb{R}^n)}, \tag{A.3a}$$

$$2\big\langle \xi_h^{n+1}, \zeta_h^n\big\rangle_{L^2(\Omega;\mathbb{R}^n)} = \big\|\xi_h^{n+1}(\cdot)\big\|^2_{L^2(\Omega;\mathbb{R}^n)} + \|\zeta_h^n(\cdot)\|^2_{L^2(\Omega;\mathbb{R}^n)} - \big\|\xi_h^{n+1}(\cdot)-\zeta_h^k(\cdot)\big\|^2_{L^2(\Omega;\mathbb{R}^n)}, \tag{A.3b}$$

gives

$$\begin{aligned} \big\|\xi_h^{n+1}(\cdot)\big\|^2_{L^2(\Omega;\mathbb{R}^n)} &= (1-\lambda)\big\|\xi_h^{n+1}(\cdot)-\xi_h^n(\cdot)\big\|^2_{L^2(\Omega;\mathbb{R}^n)} + \lambda\big\|\xi_h^{n+1}(\cdot)-\zeta_h^n(\cdot)\big\|^2_{L^2(\Omega;\mathbb{R}^n)} \\ &+ \frac{(1-\lambda)^2}{\lambda}\|\xi_h^n(\cdot)\|^2_{L^2(\Omega;\mathbb{R}^n)} + (\lambda-1)\|\zeta_h^n(\cdot)\|^2_{L^2(\Omega;\mathbb{R}^n)} + \frac{4\lambda-2\lambda^2-1}{\lambda}\langle \xi_h^n, \zeta_h^n\rangle_{L^2(\Omega;\mathbb{R}^n)} \\ &+ \lambda\delta t\left\langle A_h^{n+\lambda}\left(\frac{1-\lambda}{\lambda}\xi_h^n+\zeta_h^n\right), \frac{1-\lambda}{\lambda}\xi_h^n+\zeta_h^n\right\rangle_{L^2(\Omega;\mathbb{R}^n)} \\ &- \lambda\delta t\left\langle \beta_h^n, \frac{1-\lambda}{\lambda}\xi_h^n+\zeta_h^n\right\rangle_{L^2(\Omega;\mathbb{R}^n)}. \end{aligned} \tag{A.4}$$

Hence, multiplying equation (A.1) by $(2\lambda-1)/\lambda$ and adding the resulting expression to the above (A.4) provides

$$\begin{aligned} \big\|\xi_h^{n+1}(\cdot)\big\|^2_{L^2(\Omega;\mathbb{R}^n)} &= (1-\lambda)\big\|\xi_h^{n+1}(\cdot)-\xi_h^n(\cdot)\big\|^2_{L^2(\Omega;\mathbb{R}^n)} + \lambda\big\|\xi_h^{n+1}(\cdot)-\zeta_h^n(\cdot)\big\|^2_{L^2(\Omega;\mathbb{R}^n)} \\ &+ \lambda\|\xi_h^n(\cdot)\|^2_{L^2(\Omega;\mathbb{R}^n)} + (\lambda-1)\|\zeta_h^n(\cdot)\|^2_{L^2(\Omega;\mathbb{R}^n)} + 2(1-\lambda)\langle \xi_h^n, \zeta_h^n\rangle_{L^2(\Omega;\mathbb{R}^n)} \\ &+ \frac{2\lambda-1}{\lambda}\delta t\langle A_h^n\xi_h^n, \xi_h^n\rangle_{L^2(\Omega;\mathbb{R}^n)} - \frac{2\lambda-1}{\lambda}\delta t\langle \alpha_h^n, \xi_h^n\rangle_{L^2(\Omega;\mathbb{R}^n)} \\ &+ \lambda\delta t\left\langle A_h^{n+\lambda}\left(\frac{1-\lambda}{\lambda}\xi_h^n+\zeta_h^n\right), \frac{1-\lambda}{\lambda}\xi_h^n+\zeta_h^n\right\rangle_{L^2(\Omega;\mathbb{R}^n)} \\ &- \lambda\delta t\left\langle \beta_h^n, \frac{1-\lambda}{\lambda}\xi_h^n+\zeta_h^n\right\rangle_{L^2(\Omega;\mathbb{R}^n)}. \end{aligned} \tag{A.5}$$

Resorting to Young's inequality for products to bound the term $\langle \xi_h^n, \zeta_h^n \rangle_{L^2(\Omega;\mathbb{R}^n)}$ yields then

$$\begin{aligned}\left\|\xi_h^{n+1}(\cdot)\right\|^2_{L^2(\Omega;\mathbb{R}^n)} &= (1-\lambda)\left\|\xi_h^{n+1}(\cdot)-\xi_h^n(\cdot)\right\|^2_{L^2(\Omega;\mathbb{R}^n)} + \lambda\left\|\xi_h^{n+1}(\cdot)-\zeta_h^n(\cdot)\right\|^2_{L^2(\Omega;\mathbb{R}^n)} \\ &\quad + \|\xi_h^n(\cdot)\|^2_{L^2(\Omega;\mathbb{R}^n)} + \frac{2\lambda-1}{\lambda}\delta t\langle A_h^n\xi_h^n, \xi_h^n\rangle_{L^2(\Omega;\mathbb{R}^n)} - \frac{2\lambda-1}{\lambda}\delta t\langle \alpha_h^n, \xi_h^n\rangle_{L^2(\Omega;\mathbb{R}^n)} \\ &\quad + \lambda\delta t\left\langle A_h^{n+\lambda}\left(\frac{1-\lambda}{\lambda}\xi_h^n+\zeta_h^n\right), \frac{1-\lambda}{\lambda}\xi_h^n+\zeta_h^n\right\rangle_{L^2(\Omega;\mathbb{R}^n)} \\ &\quad - \lambda\delta t\left\langle \beta_h^n, \frac{1-\lambda}{\lambda}\xi_h^n+\zeta_h^n\right\rangle_{L^2(\Omega;\mathbb{R}^n)}.\end{aligned} \tag{A.6}$$

Finally, recalling the quasi-disspativity property (59) of the discrete operator $(A_h(t), V_{h\star})$ proved in Lemma 3.4 leads to the desired result. □

A.2. Proof of Lemma 4.3

The proof of Lemma 4.3 is given below.

Proof of Lemma 4.3. The proof involves four different steps. First, it is shown that

$$\|A_h(t)v(\cdot)\|_{L^2(\Omega;\mathbb{R}^n)} \lesssim \sqrt{\frac{\eta_c}{h}}\,\|v(\cdot)\|_{\star\star}, \qquad \text{for } v \in V_{h\star}. \tag{A.7}$$

To this end, from the definition of the norm $\|\cdot\|_{\star\star}$ according to equation (98) and Assumption 3.2, it may be deduced that

$$\begin{aligned}\langle A_h(t)v, w_h\rangle_{L^2(\Omega;\mathbb{R}^n)} &\lesssim \left(\frac{1}{t_c}\|v(\cdot)\|_{L^2(\Omega;\mathbb{R}^n)} + \eta_c\|\nabla_h v(\cdot)\|_{L^2(\Omega;\mathbb{R}^n)} + \sqrt{\varepsilon_h}\,|v(\cdot)|_\eta\right)\|w_h(\cdot)\|_{L^2(\Omega;\mathbb{R}^n)} \\ &\quad + |v(\cdot)|_\eta\,|w_h(\cdot)|_\eta + |v(\cdot)|_\eta\left(\sum_{F\in\mathcal{F}_h^i}\int_F |a(x,t)\cdot\nu_F(x)|\,\{\!\{w_h(x)\}\!\}\,\mathrm{d}x\right)^{1/2} \\ &\lesssim \left(\frac{1}{t_c}\|v(\cdot)\|_{L^2(\Omega;\mathbb{R}^n)} + \eta_c\|\nabla_h v(\cdot)\|_{L^2(\Omega;\mathbb{R}^n)} + \sqrt{\frac{\eta_c}{h}}\,|v(\cdot)|_\eta\right)\|w_h(\cdot)\|_{L^2(\Omega;\mathbb{R}^n)} \\ &\lesssim \sqrt{\frac{\eta_c}{h}}\,\|v(\cdot)\|_{\star\star}\,\|w_h(\cdot)\|_{L^2(\Omega;\mathbb{R}^n)}, \quad \text{for } (v,w_h)\in V_{h\star}\times V_h.\end{aligned} \tag{A.8}$$

Since

$$\|A_h(t)v(\cdot)\|_{L^2(\Omega;\mathbb{R}^n)} = \sup_{w_h\in V_h\setminus\{0\}}\frac{\langle A_h(t)v, w_h\rangle_{L^2(\Omega;\mathbb{R}^n)}}{\|w_h(\cdot)\|_{L^2(\Omega;\mathbb{R}^n)}}, \tag{A.9}$$

equation (A.8) provides (A.7). Moreover, applying the inverse and trace inequalities ([38], Lems. 1.44 and 1.46), yields

$$\|v_h(\cdot)\|_{\star\star} \lesssim \sqrt{\frac{\eta_c}{h}}\,\|v_h(\cdot)\|_{L^2(\Omega;\mathbb{R}^n)}, \qquad \text{for } v\in V_h, \tag{A.10}$$

which, combined with equation (A.7), leads to

$$\|A_h(t)v_h(\cdot)\|_{L^2(\Omega;\mathbb{R}^n)} \lesssim \frac{\eta_c}{h}\,\|v_h(\cdot)\|_{L^2(\Omega;\mathbb{R}^n)}, \qquad \text{for } v\in V_h. \tag{A.11}$$

The next step consists in deriving upper bounds for the terms $\alpha_h^n(x)$ and $\beta_h^n(x)$. Concerning the first quantity, the bound in equation (A.7) and the usual CFL condition (71) imply

$$\sqrt{\delta t}\,\|\alpha_h^n(\cdot)\|_{L^2(\Omega;\mathbb{R}^n)} \lesssim \|\xi_\pi^n(\cdot)\|_{\star\star} \leq \mathscr{E}_h^n. \tag{A.12}$$

Moving to the analysis of the term $\beta_h^n(x)$, using the triangle inequality gives

$$\begin{aligned}\|\beta_h^n(\cdot)\|_{L^2(\Omega;\mathbb{R}^n)} \leq{}& \left(\frac{1}{\lambda}-1\right)\left\|A_h^{n+\lambda}\xi_\pi^n(\cdot)\right\|_{L^2(\Omega;\mathbb{R}^n)} + \left\|A_h^{n+\lambda}\zeta_\pi^n(\cdot)\right\|_{L^2(\Omega;\mathbb{R}^n)}\\ &+ \delta t\,\|\pi_h\Lambda^n u^n(\cdot)\|_{L^2(\Omega;\mathbb{R}^n)} + \delta t\,\|\pi_h F^n(\cdot)\|_{L^2(\Omega;\mathbb{R}^n)}\\ &+ \lambda\delta t^2\left\|\pi_h\frac{\partial A^n}{\partial t}\frac{\partial u^n}{\partial t}(\cdot)\right\|_{L^2(\Omega;\mathbb{R}^n)} + \lambda\delta t^2\left\|\Lambda^n\frac{\partial u^n}{\partial t}(\cdot)\right\|_{L^2(\Omega;\mathbb{R}^n)} + \|\pi_h\theta^n(\cdot)\|_{L^2(\Omega;\mathbb{R}^n)}.\end{aligned} \tag{A.13}$$

The first two terms appearing in equation (A.13) may be bounded as

$$\sqrt{\delta t}\left\|A_h^{n+\lambda}\xi_\pi^n(\cdot)\right\|_{L^2(\Omega;\mathbb{R}^n)} \lesssim \|\xi_\pi^n(\cdot)\|_{\star\star}, \tag{A.14a}$$

$$\sqrt{\delta t}\left\|A_h^{n+\lambda}\zeta_\pi^n(\cdot)\right\|_{L^2(\Omega;\mathbb{R}^n)} \lesssim \|\zeta_\pi^n(\cdot)\|_{\star\star}. \tag{A.14b}$$

Moreover, it may be easily inferred that

$$\|\pi_h F^n(\cdot)\|_{L^2(\Omega;\mathbb{R}^n)} \leq \|F^n(\cdot)\|_{L^2(\Omega;\mathbb{R}^n)} \lesssim \lambda\delta t\left\|\frac{\partial^2 f(\cdot,t)}{\partial t^2}\right\|_{C^0([0,T];L^2(\Omega;\mathbb{R}^n))}, \tag{A.15a}$$

$$\|\pi_h\theta^n(\cdot)\|_{L^2(\Omega;\mathbb{R}^n)} \leq \|\theta^n(\cdot)\|_{L^2(\Omega;\mathbb{R}^n)} \lesssim \delta t^2\left\|\frac{\partial^3 u(\cdot,t)}{\partial t^3}\right\|_{C^0([0,T];L^2(\Omega;\mathbb{R}^n))}. \tag{A.15b}$$

Finally, the third, second last and third last terms may instead be bounded as

$$\|\Lambda^n u^n(\cdot)\|_{L^2(\Omega;\mathbb{R}^n)} \lesssim \lambda\delta t\eta_2\,\|u(\cdot,\cdot)\|_{C^0([0,T];H^1(\Omega;\mathbb{R}^n))}, \tag{A.16a}$$

$$\left\|\Lambda^n\frac{\partial u^n}{\partial t}(\cdot)\right\|_{L^2(\Omega;\mathbb{R}^n)} \lesssim \lambda\delta t\eta_2\left\|\frac{\partial u(\cdot,\cdot)}{\partial t}\right\|_{C^0([0,T];H^1(\Omega;\mathbb{R}^n))}, \tag{A.16b}$$

$$\left\|\pi_h\frac{\partial A^n}{\partial t}\frac{\partial u^n}{\partial t}(\cdot)\right\|_{L^2(\Omega;\mathbb{R}^n)} \lesssim \eta_1\left\|\frac{\partial u(\cdot,\cdot)}{\partial t}\right\|_{C^0([0,T];H^1(\Omega;\mathbb{R}^n))}. \tag{A.16c}$$

Combining all the above estimates and recalling that $t \leq t_\star$ therefore yields

$$\sqrt{\delta t}\,\|\beta_h^n(\cdot)\|_{L^2(\Omega;\mathbb{R}^n)} \lesssim \|\xi_\pi^n(\cdot)\|_{\star\star} + \|\zeta_\pi^n(\cdot)\|_{\star\star} + \sqrt{t}\big(C_{fu}\delta t^2 + C_u\delta t^3\big) \leq \mathscr{E}_h^n, \tag{A.17}$$

with the constants C_{fu} and C_u defined according to equation (80). Next, it is necessary to bound the term $\zeta_h^n(x)$. Starting with the error equation (87a), and resorting to the triangle inequality, the bounds (A.11) and (A.12) and the usual CFL condition (71) provides

$$\begin{aligned}\|\zeta_h^n(\cdot)\|_{L^2(\Omega;\mathbb{R}^n)} &\leq \|\xi_h^n(\cdot)\|_{L^2(\Omega;\mathbb{R}^n)} + \delta t\,\|A_h^n\zeta_h^n(\cdot)\|_{L^2(\Omega;\mathbb{R}^n)} + \delta t\,\|\alpha_h^n(\cdot)\|_{L^2(\Omega;\mathbb{R}^n)}\\ &\leq \|\xi_h^n(\cdot)\|_{L^2(\Omega;\mathbb{R}^n)} + \delta t\frac{\eta_c}{h}\,\|\xi_h^n(\cdot)\|_{L^2(\Omega;\mathbb{R}^n)} + \sqrt{\delta t}\,\|\xi_\pi^n(\cdot)\|_{\star\star}\\ &\lesssim \|\xi_h^n(\cdot)\|_{L^2(\Omega;\mathbb{R}^n)} + \sqrt{\delta t}\,\|\xi_\pi^n(\cdot)\|_{\star\star}.\end{aligned} \tag{A.18}$$

Since $\delta t \leq t_\star \leq t_c$, the above expression gives finally

$$\frac{\delta t}{t_c}\,\|\zeta_h^n(\cdot)\|^2_{L^2(\Omega;\mathbb{R}^n)} \leq \frac{\delta t}{t_c}\,\|\xi_h^n(\cdot)\|^2_{L^2(\Omega;\mathbb{R}^n)} + \delta t\,\|\xi_\pi^n(\cdot)\|^2_{\star\star}. \tag{A.19}$$

Lastly, bounds on the quantities $\delta t\langle \alpha_h^n, \xi_h^n\rangle$ and $\delta t\langle \beta_h^n, (1-\lambda)/\lambda \xi_h^n + \zeta_h^n\rangle$ should be deduced. Using the boundedness on orthogonal subscales (60) stated in Proposition 3.1, it is first possible to infer that

$$\delta t\langle \alpha_h^n, \xi_h^n\rangle \triangleq \delta t\langle A_h^n \xi_\pi^n, \xi_h^n\rangle \lesssim \delta t \left\|\xi_\pi^n(\cdot)\right\|_{\star\star} \left\|\xi_h^n(\cdot)\right\|_h \lesssim \delta t \left\|\xi_\pi^n(\cdot)\right\|_{\star\star} \left(\left|\xi_h^n(\cdot)\right|_\eta + \frac{1}{\sqrt{t_c}} \left\|\xi_h^n(\cdot)\right\|_{L^2(\Omega;\mathbb{R}^n)} \right). \tag{A.20}$$

Hence, an application of Young's inequality for product yields

$$\delta t\langle \alpha_h^n, \xi_h^n\rangle - \frac{\delta t}{2} \left|\xi_h^n(\cdot)\right|_\eta^2 \lesssim \delta t \left\|\xi_\pi^n(\cdot)\right\|_{\star\star}^2 + \frac{\delta t}{t_c} \left\|\xi_h^n(\cdot)\right\|_{L^2(\Omega;\mathbb{R}^n)}^2 \leq \delta t (\mathscr{E}_h^n)^2. \tag{A.21}$$

Similarly, resorting again to equation (60), the bound previously deduced according to (A.17), and Cauchy–Schwarz' inequality provides

$$\begin{aligned} \delta t \left\langle \beta_h^n, \frac{1-\lambda}{\lambda}\xi_h^n + \zeta_h^n \right\rangle_{L^2(\Omega;\mathbb{R}^n)} &\lesssim \delta t \left\| \frac{1-\lambda}{\lambda}\xi_\pi^n(\cdot) + \zeta_\pi^n(\cdot) \right\|_{\star\star} \left\| \frac{1-\lambda}{\lambda}\xi_h^n(\cdot) + \zeta_h^n(\cdot) \right\|_h \\ &\quad + \delta t \big(C_{fu}\delta t^2 + C_u \delta t^3\big) \left\| \frac{1-\lambda}{\lambda}\xi_h^n(\cdot) + \zeta_h^n(\cdot) \right\|_{L^2(\Omega;\mathbb{R}^n)} \\ &\lesssim \delta t \left(\frac{1-\lambda}{\lambda} \left\|\xi_\pi^n(\cdot)\right\|_{\star\star} + \left\|\zeta_\pi^n(\cdot)\right\|_{\star\star} \right) \\ &\quad \times \left(\left| \frac{1-\lambda}{\lambda}\xi_h^n(\cdot) + \zeta_h^n(\cdot) \right|_\eta + \frac{1}{\sqrt{t_c}} \left\| \frac{1-\lambda}{\lambda}\xi_h^n(\cdot) + \zeta_h^n(\cdot) \right\|_{L^2(\Omega;\mathbb{R}^n)} \right) \\ &\quad + \delta t \big(C_{fu}\delta t^2 + C_u \delta t^3\big) \left\| \frac{1-\lambda}{\lambda}\xi_h^n(\cdot) + \zeta_h^n(\cdot) \right\|_{L^2(\Omega;\mathbb{R}^n)}. \end{aligned} \tag{A.22}$$

Using again Young's inequality for product therefore gives

$$\begin{aligned} \delta t \left\langle \beta_h^n, \frac{1-\lambda}{\lambda}\xi_h^n + \zeta_h^n \right\rangle_{L^2(\Omega;\mathbb{R}^n)} - \frac{\delta t}{2} \left| \frac{1-\lambda}{\lambda}\xi_h^n(\cdot) + \zeta_h^n(\cdot) \right|_\eta^2 &\lesssim \delta t \left(\left\|\xi_\pi^n(\cdot)\right\|_{\star\star}^2 + \left\|\zeta_\pi^n(\cdot)\right\|_{\star\star}^2 \right) \\ &\quad + \frac{\delta t}{t_c} \left(\left\|\xi_h^n(\cdot)\right\|_{L^2(\Omega;\mathbb{R}^n)}^2 + \left\|\zeta_h^n(\cdot)\right\|_{L^2(\Omega;\mathbb{R}^n)}^2 \right) \\ &\quad + \delta t \big(C_{fu}\delta t^2 + C_u \delta t^3\big) \left(\left\|\xi_h^n(\cdot)\right\|_{L^2(\Omega;\mathbb{R}^n)} + \left\|\zeta_h^n(\cdot)\right\|_{L^2(\Omega;\mathbb{R}^n)} \right). \end{aligned} \tag{A.23}$$

Invoking the estimate (A.18) to bound the terms involving $\left\|\zeta_h^n(\cdot)\right\|_{L^2(\Omega;\mathbb{R}^n)}$, it may be finally deduced that

$$\delta t \left\langle \beta_h^n, \frac{1-\lambda}{\lambda}\xi_h^n + \zeta_h^n \right\rangle_{L^2(\Omega;\mathbb{R}^n)} - \frac{\delta t}{2} \left| \frac{1-\lambda}{\lambda}\xi_h^n(\cdot) + \zeta_h^n(\cdot) \right|_\eta^2 \lesssim \delta t (\mathscr{E}_h^n)^2. \tag{A.24}$$

Recalling that $\omega_h \leq 1/t_c \leq 1/t_\star$, collecting the above bounds and inserting them into equation (97) leads to the desired result. □

Appendix B. Some numerical results concerning RK3 schemes

RK3 schemes enjoy stronger stability properties than their lower-order counterparts. Moreover, quasi-optimal convergence rates may be deduced owing to less stringent CFL conditions. For example, in [38], limited to the case of IBVPs with constant coefficients, it is found that the classic CFL condition is sufficient to derive quasi-optimal error estimates. To investigate the potential of RK3 schemes when it comes to time-varying problems, numerical experiments have been performed concerning Heun's third-order algorithm considering

TABLE B.1. Convergence of the total error for different polynomial degrees $k = 1$ and 2 and Heun's third-order scheme, concerning the IBVP considered in Section 5.1.2.

Meshsize h	Total error ($k = 1$, 1-CFL)	Total error ($k = 2$, 1-CFL)
0.05	$1.70 \cdot 10^{-3}$	$1.32 \cdot 10^{-3}$
0.025	$8.51 \cdot 10^{-4}$	$6.55 \cdot 10^{-3}$
0.0125	$3.92 \cdot 10^{-4}$	$3.21 \cdot 10^{-4}$
Meshsize h	Total error ($k = 1$, 4/3-CFL)	Total error ($k = 2$, 4/3-CFL)
0.05	$9.93 \cdot 10^{-3}$	$9.93 \cdot 10^{-3}$
0.025	$3.93 \cdot 10^{-3}$	$3.91 \cdot 10^{-3}$
0.0125	$2.31 \cdot 10^{-3}$	$1.50 \cdot 10^{-4}$
Meshsize h	Total error ($k = 1$, 2-CFL)	Total error ($k = 2$, 2-CFL)
0.05	$1.61 \cdot 10^{-3}$	$9.47 \cdot 10^{-4}$
0.025	$5.65 \cdot 10^{-4}$	$1.53 \cdot 10^{-4}$
0.0125	$2.24 \cdot 10^{-4}$	$2.84 \cdot 10^{-5}$

the IBVP described in Section 5.1.2, but with the original IC (111b) replaced with $u_0(x) = x^4$ to ensure $C^4([0,T];L^2(\Omega;\mathbb{R}^n)) \cap C^1([0,T];H^1(\Omega;\mathbb{R}^n))$ regularity for the exact solution (see [38], Thm. 3.13). The total error, calculated according to equation (3.29) in [38], is reported in Table B.1 and illustrated in Figure B.1 for the three different CFL conditions and corresponding values of the parameter $\varrho = 0.05$, 0.5, and 1, respectively. It appears that, for $k = 1$, the classic CFL condition is not sufficient to ensure quasi-optimal convergence rates, whereas the higher-order ones follow a similar trend to $O(h^{3/2})$ (this might perhaps be ascribed to the peculiar combination of the RK3 scheme with the low polynomial degree $k = 1$). On the other hand, for $k = 2$, the 2-CFL condition seems to be the only one ensuring a quasi-optimal convergence rate. In any case, the results point out at the possibility of overcoming some of the limitations encountered in the present work by adopting higher-order RK algorithms for time discretization.

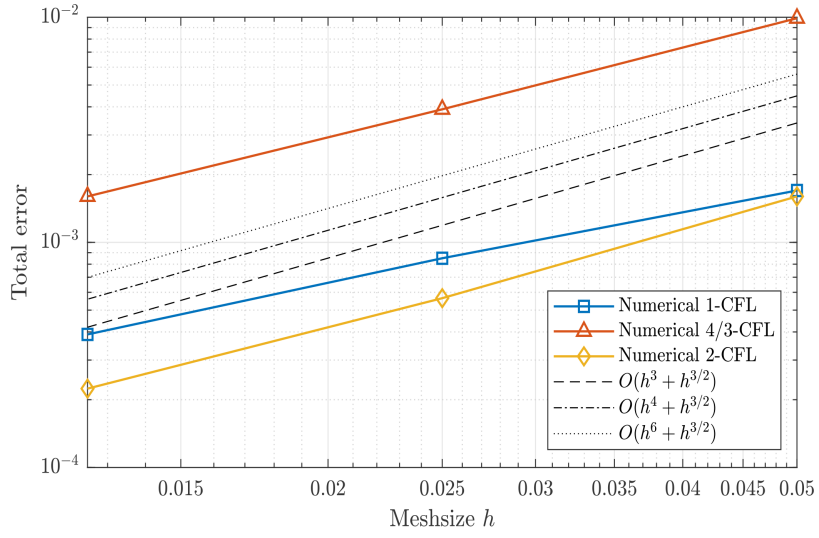

(a)

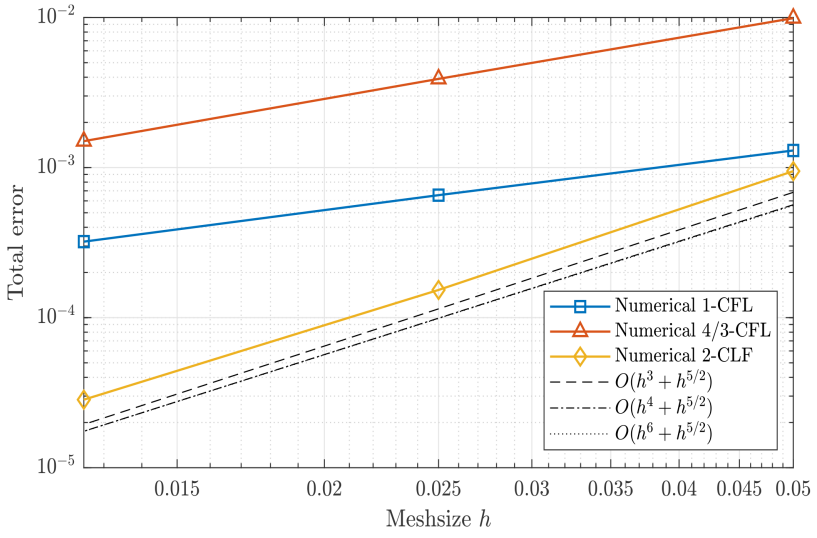

(b)

FIGURE B.1. Convergence of the total error for different polynomial degrees $k = 1$ and 2 and Heun's third-order scheme, concerning the IBVP considered in Section 5.1.2. (a) Convergence of the total error for Heun's third-order scheme (polynomial degree $k = 1$). (b) Convergence of the total error for Heun's third-order scheme (polynomial degree $k = 2$).

AUTHOR CONTRIBUTION STATEMENT

Luigi Romano: Conceptualisation, Theory, Formal analysis, Investigation, Methodology, Implementation, Visualisation, Writing – original draft; ***Axel Målqvist***: Theory, Supervision. All the authors read and approved the original version of the manuscript.

References

[1] L.C. Evans, Partial Differential Equations, 2nd edition. American Mathematical Society (1996).

[2] S. Larsson and V. Thomee, Partial Differential Equations with Numerical Methods, 1st edition. Springer, Berlin, Heidelberg (2009).

[3] K.L. Johnson, Contact Mechanics. Cambridge University Press (1985).

[4] I.G. Goryacheva, Contact Mechanics in Tribology. Springer Science & Business Media (1998).

[5] J.J. Kalker, *On the rolling contact of two elastic bodies in the presence of dry friction*. Dissertation, TH Delft, Delft (1967).

[6] J.J. Kalker, Three-Dimensional Elastic Bodies in Rolling Contact. Springer, Dordrecht (1990).

[7] M. Guiggiani, The Science of Vehicle Dynamics, 2nd edition. Springer International, Cham, Switzerland (2018).

[8] H.B. Pacejka, Tire and Vehicle Dynamics, 3rd edition. Elsevier/BH, Amsterdam (2012).

[9] F. Frendo and F. Bucchi, "Brush model" for the analysis of flat belt transmissions in steady-state conditions, in Mechanism and Machine Theory. Vol. 143. Elseiver (2020) 103653.

[10] F. Frendo and F. Bucchi, Enhanced brush model for the mechanics of power transmission in flat belt drives under steady-state conditions: effect of belt elasticity, in Mechanism and Machine Theory. Vol. 153. Elseiver (2020) 103998.

[11] F. Bucchi and F. Frendo, Validation of the brush model for the analysis of flat belt transmissions in steady-state conditions by finite element simulation, in Mechanism and Machine Theory. Vol. 167. Elseiver (2022) 104556.

[12] F. Marques, P. Flores, J.C. Pimenta Claro and H.M. Lankarani, A survey and comparison of several friction force models for dynamic analysis of multibody mechanical systems. *Nonlinear Dyn.* **86** (2016) 1407–1443.

[13] F. Marques, P. Flores, J.C. Pimenta Claro and H.M. Lankarani, Modeling and analysis of friction including rolling effects in multibody dynamics: a review. *Multibody Syst. Dyn.* **45** (2019) 223–244.

[14] L. Romano, F. Timpone, F. Bruzelius and B. Jacobson, Analytical results in transient brush tyre models: theory for large camber angles and classic solutions with limited friction. *Meccanica* **57** (2022) 165–191.

[15] L. Romano, F. Timpone, F. Bruzelius and B. Jacobson, Rolling, tilting and spinning spherical wheels: analytical results using the brush theory, in Mechanism and Machine Theory Mechanism and Machine Theory. Vol. 167. Elseiver (2022) 104836.

[16] L. Romano, Advanced Brush Tyre Modelling. *SpringerBriefs in Applied Sciences*. Springer, Cham (2022).

[17] J. Deur, Modeling and analysis of longitudinal tire dynamics based on the LuGre friction model. *IFAC Proc. Vol.* **34** (2001) 91–96.

[18] J. Deur, J. Asgari and D. Hrovat, A dynamic tire friction model for combined longitudinal and lateral motion, in Proceedings of the ASME-IMECE World Conference. ASME (2001).

[19] J. Deur, J. Asgari and D. Hrovat, A 3D brush-type dynamic tire friction model. *Veh. Syst. Dyn.* **42** (2004) 133–173.

[20] J. Deur, V. Ivanovic, M. Troulis, C. Miano, D. Hrovat and J. Asgari, Extensions of the LuGre tyre friction model related to variable slip speed along the contact patch length. *Veh. Syst. Dyn.* **43** (2005) 508–524.

[21] C. Canudas-de-Wit, P. Tsiotras, E. Velenis, M. Basset and G. Gissinger, Dynamic friction models for road/tire longitudinal interaction. *Veh. Syst. Dyn.* **39** (2003) 189–226.

[22] P. Tsiotras, E. Velenis and M. Sorine, A LuGre tire friction model with exact aggregate dynamics. *Veh. Syst. Dyn.* **42** (2004) 195–210.

[23] E. Velenis, P. Tsiotras, C. Canudas-de-Wit and M. Sorine, Dynamic tyre friction models for combined longitudinal and lateral vehicle motion. *Veh. Syst. Dyn.* **43** (2005) 3–29.

[24] L. Romano, F. Bruzelius and B. Jacobson, An extended LuGre-brush tyre model for large camber angles and turning speeds. *Veh. Syst. Dyn.* **61** (2022) 1674–1706.

[25] F. Marques, Ł. Woliński, M. Wojtyra, P. Flores and H.M. Lankarani, An investigation of a novel LuGre-based friction force model. *Mech. Mach. Theory* **166** (2021) 104493.

[26] J.J. Kalker, Transient phenomena in two elastic cylinders rolling over each other with dry friction. *J. Appl. Mech.* **37** (1970) 677–688.

[27] J.J. Kalker, Transient rolling contact phenomena. *ASLE Trans.* **14** (1971) 177–184.

[28] E.A.H. Vollebregt, User guide for CONTACT, Vollebregt & Kalker's rolling and sliding contact model. Techical report TR09-03, version 13.

[29] E.A.H. Vollebregt and P. Wilders, FASTSIM2: a second-order accurate frictional rolling contact algorithm. *Comput. Mech.* **47** (2011) 105–116.

[30] E.A.H. Vollebregt, S.D. Iwnicki, G. Xie and P. Shackelton, Assessing the accuracy of different simplified frictional rolling contact algorithms. *Veh. Syst. Dyn.* **50** (2012) 1–17.

[31] E.A.H. Vollebregt, Numerical modeling of measured railway creep versus creep-force curves with CONTACT. *Wear* **314** (2014) 87–95.

[32] L. Romano, F. Bruzelius and B. Jacobson, Transient tyre models with a flexible carcass. *Veh. Syst. Dyn.* **62** (2024) 1268–1307.

[33] L. Romano, M. Maglio and S. Bruni, Transient wheel-rail rolling contact theories. *Tribol. Int.* **186** (2023) 108600.

[34] B. Cockburn, S. Hou and C.W. Shu, The Runge–Kutta local projection discontinuous Galerkin finite element method for conservation laws. IV. The multidimensional case. *Math. Comp.* **54** (1990) 545–581.

[35] B. Cockburn, G.E. Karniadakis and C.W. Shu, Discontinuous Galerkin Methods – Theory, Computation and Applications. Vol. 11 of *Lecture Notes in Computer Science and Engineering*. Springer (2000).

[36] B. Cockburn, S. Lin and C.W. Shu, TVB Runge–Kutta local projection discontinuous Galerkin finite element method for conservation laws. III. One-dimensional systems. *J. Comput. Phys.* **84** (1989) 90–113.

[37] B. Cockburn and C.W. Shu, TVB Runge–Kutta local projection discontinuous Galerkin finite element method for conservation laws. II. General framework. *Math. Comp.* **52** (1989) 411–435.

[38] D.A. Di Pietro and A. Ern, Mathematical Aspects of Discontinuous Galerkin Methods, 1st edition. Springer Berlin, Heidelberg (2011).

[39] E. Burman, E. Ern and M.A. Fernández, Explicit Runge–Kutta schemes and finite elements with symmetric stabilization for first-order linear PDE systems. *SIAM J. Numer. Anal.* **48** (2010) 2019–2042.

[40] F.J. Massey, Abstract evolution equations and the mixed problem for symmetric hyperbolic systems. *Trans. Am. Math. Soc.* **168** (1972) 165–188.

[41] T. Kato, Linear evolution equations of "hyperbolic" type. *J. Fac. Sci. Univ. Tokyo* **17** (1970) 241–258.

[42] T. Kato, Perturbation Theory for Linear Operators, 2nd edition. Springer Berlin, Heidelberg (1995).

[43] A.E. Taylor, Introduction to Functional Analysis. Wiley, New York (1958).

[44] R.F. Curtain and H. Zwart, An Introduction to Infinite-Dimensional Linear Systems Theory, 1st edition. Springer New York, NY (2012).

[45] R.F. Curtain and H. Zwart, Introduction to Infinite-Dimensional Systems Theory: A State-Space Approach, 1st edition. Springer, New York, NY (2020).

[46] H. Tanabe, Equations of Evolution, 1st edition. Pitman (1979).

[47] H. Tanabe, Functional Analytic Methods for Partial Differential Equations, 1st edition. CRC Press (1997).

[48] A. Pazy, Semigroups of Linear Operators and Applications to Partial Differential Equations, 1st edition. Springer New York, NY (1983).

[49] C. Bardos, Problèmes aux limites pour les équations aux dérivées partielles du premier ordre à coefficients réels, théorèmes d'approximation application à l'équation de transport. *Ann. Sci. Éc. Norm. Super.* **4** (1970) 185–233.

[50] H.O. Kreiss and J. Lorenz, Initial-Boundary Value Problems and the Navier–Stokes Equations. Society for Industrial and Applied Mathematics (2004).

[51] B. Gustafsson, H.O. Kreiss and J. Oliger, Time-Dependent Problems and Difference Methods, 2nd edition. Wiley, Pure and Applied Mathematics (2013).

[52] S. Benzoni-Gavage and D. Serre, Multi-Dimensional Hyperbolic Partial Differential Equations: First-Order Systems and Applications, 1st edition. Oxford Academic (2006).

[53] G. Crippa, C. Donadello and L.V. Spinolo, Initial-boundary value problems for continuity equations with BV coefficients. *J. Math. App.* **102** (2022) 79–98.

[54] C.W. Shu and S. Osher, Efficient implementation of essentially nonoscillatory shock-capturing schemes. *J. Comput. Phys.* **77** (19988) 439–471.

[55] M. Ciavarella and J. Barber, Influence of longitudinal creepage and wheel inertia on short-pitch corrugation: a resonance-free mechanism to explain the roaring rail phenomenon. *Proc. Inst. Mech. Eng. Part J: J. Eng. Tribol.* **222** (2008) 171–181.

[56] L. Afferrante and M. Ciavarella, Short-pitch rail corrugation: a possible resonance-free regime as a step forward to explain the "enigma"? *Wear* **266** (2009) 934–944.

[57] L. Afferrante and M. Ciavarella, Short pitch corrugation of railway tracks with wooden or concrete sleepers: An enigma solved? *Tribol. Int.* **43** (2010) 610–622.